AD NUMBER

ADB205180

NEW LIMITATION CHANGE

TO

Approved for public release, distribution unlimited

FROM

Distribution authorized to DoD only; Specific Authority; Oct 95. Other requests shall be referred to Commander, U.S. Army Medical Research and Material Command, Attn: MCMR-RMI-S, Ft. Detrick, MD 21702-5012.

AUTHORITY

USAMRMC ltr dtd 21 Jan 2000

AD_____

CONTRACT NUMBER: DAMD17-95-C-5043

TITLE: Lightweight Portable, Noninvasive Physiologic Sensors for Multisite Determination/Quantitation of Surface and Deep Tissue Microvascular Blood Flow

PRINCIPAL INVESTIGATOR: Beth Schrope, Ph.D.

CONTRACTING ORGANIZATION: Reshet Incorporated
Philadelphia, Pennsylvania 19104

REPORT DATE: October 1995

TYPE OF REPORT: Final, Phase I

PREPARED FOR: U.S. Army Medical Research and Materiel Command
Fort Detrick, Maryland 21702-5012

REPORT DOCUMENTATION PAGE

Form Approved
OMB No. 0704-0188

1. AGENCY USE ONLY *(Leave blank)*	2. REPORT DATE	3. REPORT TYPE AND DATES COVERED
	October 1995	Final, Phase I 15 Mar 95 - 14 Sep 95

4. TITLE AND SUBTITLE
Lightweight Portable, Noninvasive Physiologic Sensors for Multisite Determination/Quantitation of Surface and Deep Tissue Microvascular Blood Flow

5. FUNDING NUMBERS
DAMD17-95-C-5043

6. AUTHOR(S)
Beth Schrope, Ph.D.

7. PERFORMING ORGANIZATION NAME(S) AND ADDRESS(ES)
Reshet Incorporated
Philadelphia, Pennsylvania 19104

8. PERFORMING ORGANIZATION REPORT NUMBER

9. SPONSORING/MONITORING AGENCY NAME(S) AND ADDRESS(ES)
U.S. Army Medical Research and Materiel Command
Fort Detrick, Maryland 21702-5012

10. SPONSORING/MONITORING AGENCY REPORT NUMBER

11. SUPPLEMENTARY NOTES

12a. DISTRIBUTION/AVAILABILITY STATEMENT
Distribution authorized to DoD components only, Specific Authority. Other requests shall be forwarded to the Commander, U.S. Army Medical Research and Materiel Command, ATTN: MCMR-RMI-S, Fort Detrick, Maryland 21702-5012

Oct 95

12b. DISTRIBUTION CODE

13. ABSTRACT *(Maximum 200 words)*

Detecting, measuring and quantifying blood perfusion in the human tissues is a significant problem not well characterized by today's instruments. Tissue perfusion, or blood flow in the microcirculation, is an important indicator of the relative health of tissue, relating directly to tissue oxygenation and nutrition, as well as toxic metabolite removal. In this Phase I project we endeavored to answer this need with a new technology involving the ultrasound detection and quantification of this parameter, utilizing a harmless, injectable contrast agent. We designed and tested a system for this method, and serendipitously discovered and developed an alternate method that may prove to be more robust than the original one proposed.

14. SUBJECT TERMS
ultrasound, perfusion, microcirculation, second harmonic, blood flow, noninvasive, shadowing

15. NUMBER OF PAGES
39

16. PRICE CODE

17. SECURITY CLASSIFICATION OF REPORT	18. SECURITY CLASSIFICATION OF THIS PAGE	19. SECURITY CLASSIFICATION OF ABSTRACT	20. LIMITATION OF ABSTRACT
Unclassified	Unclassified	Unclassified	limited

GENERAL INSTRUCTIONS FOR COMPLETING SF 298

The Report Documentation Page (RDP) is used in announcing and cataloging reports. It is important that this information be consistent with the rest of the report, particularly the cover and title page. Instructions for filling in each block of the form follow. It is important to ***stay within the lines*** to meet ***optical scanning requirements***.

Block 1. Agency Use Only *(Leave blank)*.

Block 2. Report Date. Full publication date including day, month, and year, if available (e.g. 1 Jan 88). Must cite at least the year.

Block 3. Type of Report and Dates Covered. State whether report is interim, final, etc. If applicable, enter inclusive report dates (e.g. 10 Jun 87 - 30 Jun 88).

Block 4. Title and Subtitle. A title is taken from the part of the report that provides the most meaningful and complete information. When a report is prepared in more than one volume, repeat the primary title, add volume number, and include subtitle for the specific volume. On classified documents enter the title classification in parentheses.

Block 5. Funding Numbers. To include contract and grant numbers; may include program element number(s), project number(s), task number(s), and work unit number(s). Use the following labels:

C	- Contract	**PR**	- Project
G	- Grant	**TA**	- Task
PE	- Program Element	**WU**	- Work Unit Accession No.

Block 6. Author(s). Name(s) of person(s) responsible for writing the report, performing the research, or credited with the content of the report. If editor or compiler, this should follow the name(s).

Block 7. Performing Organization Name(s) and Address(es). Self-explanatory.

Block 8. Performing Organization Report Number. Enter the unique alphanumeric report number(s) assigned by the organization performing the report.

Block 9. Sponsoring/Monitoring Agency Name(s) and Address(es). Self-explanatory.

Block 10. Sponsoring/Monitoring Agency Report Number. *(If known)*

Block 11. Supplementary Notes. Enter information not included elsewhere such as: Prepared in cooperation with...; Trans. of...; To be published in.... When a report is revised, include a statement whether the new report supersedes or supplements the older report.

Block 12a. Distribution/Availability Statement. Denotes public availability or limitations. Cite any availability to the public. Enter additional limitations or special markings in all capitals (e.g. NOFORN, REL, ITAR).

- **DOD** - See DoDD 5230.24, "Distribution Statements on Technical Documents."
- **DOE** - See authorities.
- **NASA** - See Handbook NHB 2200.2.
- **NTIS** - Leave blank.

Block 12b. Distribution Code.

- **DOD** - Leave blank.
- **DOE** - Enter DOE distribution categories from the Standard Distribution for Unclassified Scientific and Technical Reports.
- **NASA** - Leave blank.
- **NTIS** - Leave blank.

Block 13. Abstract. Include a brief *(Maximum 200 words)* factual summary of the most significant information contained in the report.

Block 14. Subject Terms. Keywords or phrases identifying major subjects in the report.

Block 15. Number of Pages. Enter the total number of pages.

Block 16. Price Code. Enter appropriate price code *(NTIS only)*.

Blocks 17. - 19. Security Classifications. Self-explanatory. Enter U.S. Security Classification in accordance with U.S. Security Regulations (i.e., UNCLASSIFIED). If form contains classified information, stamp classification on the top and bottom of the page.

Block 20. Limitation of Abstract. This block must be completed to assign a limitation to the abstract. Enter either UL (unlimited) or SAR (same as report). An entry in this block is necessary if the abstract is to be limited. If blank, the abstract is assumed to be unlimited.

*U.S.GPO:1993-0-358-779

FOREWORD

Opinions, interpretations, conclusions and recommendations are those of the author and are not necessarily endorsed by the US Army.

____ Where copyrighted material is quoted, permission has been obtained to use such material.

____ Where material from documents designated for limited distribution is quoted, permission has been obtained to use the material.

____ Citations of commercial organizations and trade names in this report do not constitute an official Department of Army endorsement or approval of the products or services of these organizations.

____ In conducting research using animals, the investigator(s) adhered to the "Guide for the Care and Use of Laboratory Animals," prepared by the Committee on Care and Use of Laboratory Animals of the Institute of Laboratory Resources, National Research Council (NIH Publication No. 86-23, Revised 1985).

____ For the protection of human subjects, the investigator(s) adhered to policies of applicable Federal Law 45 CFR 46.

____ In conducting research utilizing recombinant DNA technology, the investigator(s) adhered to current guidelines promulgated by the National Institutes of Health.

____ In the conduct of research utilizing recombinant DNA, the investigator(s) adhered to the NIH Guidelines for Research Involving Recombinant DNA Molecules.

____ In the conduct of research involving hazardous organisms, the investigator(s) adhered to the CDC-NIH Guide for Biosafety in Microbiological and Biomedical Laboratories.

Robert A. Sharpe 9/21/95

PI - Signature Date

Table of Contents

I. INTRODUCTION

I.1. Statement of the Problem

The procedure of blood flow measurement is well established and extends into many areas of medical practice. Direct indication of the patient's hemodynamic status (and, less directly, the overall status) results from analysis of basic blood flow characteristics: velocity, pulsatility, resistance and so on. Vascular disorders such as plaque accumulation, stenosis or aneurysm can be diagnosed and monitored by imaging or otherwise evaluating blood flow characteristics. Quantification of large vessel blood flow is integral in determining the course of treatment for a specific disorder or patient. Current techniques used to obtain quantified flow data, however, are limited to larger blood vessels systems such as the carotids, femorals, aorta, renal and hepatic vessels, and are often restricted to the more superficially located vessels found easily by clinical exam (ie, feeling for the pulse).

Blood perfusion of tissue, that is, blood flow through the tiny microcirculation, is an important area of clinical investigation. The viability of a region of tissue is directly related to the perfusion of (and, thus, the oxygen supply available to) that region. For example, trauma to one of the large distributing vessels to a distal limb can result in underperfusion of the tissue in that region, resulting in ischemia and eventual necrosis necessitating amputation. Similarly, chronic occlusive coronary disease results in underperfusion of a region of myocardium. Early detection of the low perfusion could avoid life-endangering complications of myocardial infarction through appropriate therapy. Another example is the neovascularity characteristic of many tumors. This new vasculature supplying nutrients to the rapidly growing tissue comprises mostly small vessels which elude detection by conventional means. Unfortunately, available methods for evaluating blood perfusion lack the highly desirable characteristics of noninvasiveness and quantifiability.

An ideal blood perfusion diagnostic device for use in triage situations would be uncomplicated to use under high stress and often mobile conditions. Such a device would noninvasively supply information about the hemodynamic status of deep tissue. Accurate and precise measures would be obtained which would be immediately recognizable by, and significant to, trained personnel as reliable indicators of tissue survivability. The device would also be versatile enough to remain with a patient for extended monitoring and should be compatible with commonly used display and data storage devices. Currently no system or device meets these requirements.

Until roughly the last decade, limitations in blood flow diagnostic technologies have made analysis of blood perfusion (flow in a bed of the smallest vessels: arterioles, capillaries, venules) clinically impractical. Other noninvasive techniques addressed the desire to obtain absolute flow information from the microcirculation but were limited in robustness (e.g., plethysmography, which required a stable hemodynamic state, an appreciable amount of time to generate the data, and

awkward, bulky, somewhat fragile equipment), reliability (e.g., ^{133}Xenon clearance) and regions of measurement (e.g., thermal clearance and laser Doppler flowmetry which measure superficial flow).

Limited progress in noninvasively measuring microcirculatory flow via ultrasound has been reported. The obstacles in the way of such a diagnostic procedure derive from the physiology of the measured system: slow blood velocity and low volume. Capillary blood velocity is, characteristically, no greater than about 2 mm/sec; the relative blood volume of tissue at resting perfusion is about 1/1000th that of tissue. A Doppler system operating at 5 MHz would produce frequency deviations on the order of tens of Hertz for velocities on the order of 1 mm/sec, below the resolution of conventional systems. Also, tissue movement from either gross patient motion or from autonomic vasomotive processes can "bury" the signal of interest in artifact, particularly because of the small capillary blood volume in the measurement region (which produces a much decreased blood-to-tissue echo ratio).

Some preliminary theoretical work (Burns and Reid, 1989) has addressed the small frequency shift problem via stable oscillators. The proposed system was expected to resolve shifts of less than 10 Hertz from a 1 MHz carrier; development and tests of the system have not been published. Dymling, et al (1991), used a continuous wave Doppler system without the customary low-pass filter and reported promising results. The method is limited, however, by tissue motion artifact.

Use of a contrast agent to enhance the signal-to-clutter ratio of capillary blood flow addresses the small signal problem inherent in attempting to measure microcirculatory perfusion via Doppler ultrasound. Reports by Monaghan, et al (1988), Ong, et al (1984), Ten Cate, et al (1984) have at least demonstrated the feasibility of contrast enhancement in microcirculatory flow measurement. However, the small blood volume involved, along with tissue motion artifact, can confound the frequency shift or intensity of the Doppler signal and still lead to ambiguous results.

Another limitation of existing ultrasound techniques is lack of consistency in the measurement system. Changes in the quality of coupling between the transducer and skin or in the angle of the incident beam can cause variations in the incident and reflected ultrasonic energy. This inconsistency is inherent in all of the present systems, including those utilizing contrast enhancement. Therefore, absolute quantification of signal intensity and, thus, absolute quantification of perfusion, is not possible with current methods.

Analysis by Schrope and Newhouse (1993) demonstrated that intervening tissue produced negligible nonlinearity in the propagated signal as compared with a selected contrast agent in the capillaries. The nonlinear contrast agent generates a second harmonic component which allows elimination of the clutter signal returned at the fundamental frequency by vasomotive processes and intervening tissue. Utilizing this nonlinear contrast agent and recently developed algorithms, our

proposed system overcomes the obstacles which hindered previous methods in order to provide a technique for the unambiguous quantification of tissue blood flow measurement.

The research covered by this report is directed to developing a device which will provide an unambiguous quantitative measurement of tissue perfusion and meet the other requirements as stated in the preceding section via Doppler ultrasound techniques. Previous work (Schrope, et al, 1992; Schrope and Newhouse, 1993) demonstrated the advantage of using a nonlinear contrast agent and analyzing the resulting second harmonic component of the return signal (echo). The analysis technique greatly reduces the "clutter" produced by echoes from surrounding tissue and vasomotive processes providing a well-differentiated signal due only to blood flow. Additionally, a unique approach to the problem of quantifying the signal intensity at the target tissue and, thus the absolute measure of blood flow, will result in a calibrated system which offers useful and reliable quantitative information about deep tissue blood flow.

I.2. Phase I Goals

As delineated in the Phase I Proposal, our method of investigation in this project encompassed four technical objectives:

1. *Assess the appropriateness and technical feasibility of the second harmonic ultrasonic microcirculatory blood flow measurement in the application of trauma medicine.*

To achieve this goal we began with a detailed discussion of the "Soldier Individual Computer" project with a member of the team in the Army. We learned much more about the ultimate goals of this large project than were available in the RFP, and we were able to adjust our priorities and designs accordingly.

2. *Refine and adapt algorithms for second harmonic tissue perfusion measurement to be compatible with commonly available display and data storage devices, such as used by the military and commercial sectors.*

Again, the discussion with the Army project representative clarified this goal for the project. Specifically, we learned that the Army desired a specific data output for integration into the Soldier Individual Computer system. We endeavored to ultimately provide this output from our algorithms.

3. *Build prototype device that is economical, durable, easy-to-use and compatible with existing systems.*

As stated in the proposal, our phase I effort was not directed at "reinventing the wheel" - hence, we chose mostly off-the-shelf components for our feasibility testing system. Here we report several designs for systems that were conceived during the project period; in our experimental methods section we describe the design actually used for the experimentation and

testing. Eventually our technology and algorithms will be integrated into a small DSP computer chip and an external sensor, for integration into the Soldier Individual Computer.

4. *Test prototype on in vitro perfusion models.*

This project entailed extensive testing of the concept under question, that is, the second harmonic perfusion measurement. As will be described later in this report, we endeavored to carefully determine the useful limits of the system, in terms of frequency, contrast agent concentration, input power, etc..

II. SECOND HARMONIC SYSTEM DESIGN

In this section is a summary of several designs for a system to measure and quantify blood perfusion using the second harmonic signal detected from the region of interest. In general, we proposed three different types of systems.

Our first system, schematically demonstrated in Figure 1, is based on apparatus currently used in the laboratory with the addition of a few enhancements such as PC interface, improved precision equipment, etc.. The advantages of such a system are that: it requires minimal engineering effort, leaving more time available for extensive experimentation and understanding of the contrast agent; it is very flexible due to the general nature of the lab test equipment; it's A/D conversion and PC interface allows storage of raw data which can be saved and manipulated in the future as new and improved algorithms become available. The main disadvantage of this system, also related to its flexibility and general nature as test equipment, is its high cost.

The system depicted in Figure 2 is actually a power estimator of both the first and second harmonic. Again we convert our data to digital format for analysis; however, the A/D converters are employed at a much reduced speed of less than 1 MHz and 8 bit A/D conversion (versus at least 12 bit needed for the first approach). The main advantages of this system are: it is truly a prototype system that can lead to product design if the approach is found successful; it retains the feature of the first approach in that the first and second harmonic amplitudes can be estimated from within a specified range cell; integration of other data analysis features (for example, Doppler or the attenuation analysis to be discussed later in this report) is rather straightforward. However, this system requires significantly more engineering effort, which may not be appropriate at this stage of the research. Also, this design is less flexible than the first (mainly in controlling the characteristics of the transmitted signal such as frequency, burst length, power, etc.). Of course, these parameters could be altered by modifying the system, but in the first design the parameters could be altered continuously and within the same experiment.

Referring again to Figure 2, the details of the design are as follows. The transmitter transmits bursts at $\omega = 2\pi f$ at a given repetition rate somewhere between 500 and 2000 Hz. The received signal is amplified (amplifiers not shown) and split into two signals. In the first branch

(upper) the fundamental harmonic signal is processed, and in the second branch (lower) the second harmonic signal is processed. The signals are processed in quadrature, so restoration of the signals' envelope and with it the power are possible. We in fact created a power meter for the fundamental and second harmonic signals. In order to restore the signal power, we take the signals from the quadrature outputs and, using a lookup table, estimate the returned signal envelopes of the gate signals. Averaging of consecutive returned signals improves the robustness of the results.

Theoretically, the development is as follows. The returned signal within the gate region can be described as:

$$r(t) = A(t) \sin(\omega t + \phi) \qquad \text{(II.1)}$$

After multiplication with the two quadrature signals $\sin(\omega t)$, $\cos(\omega t)$, we obtain the following signals (after the mixer and low pass filters):

$$r_1(t) = A(t)\sin(\phi) \qquad \text{(II.2)}$$

$$r_2(t) = A(t)\cos(\phi) \qquad \text{(II.3)}$$

Restoration of A(t) is easily achievable through

$$A(t) = (r_1^2(t) + r_2^2(t))^{0.5} \qquad \text{(II.4)}$$

which can best be accomplished via lookup tables. From A(t) we estimate its average within the gate. The same analysis applies to the second harmonic signals. Note that the 0.5 MHz filters are anti-aliasing filters and their function is to retain the original information contained in the returned signals for the fundamental harmonic in the upper branch and the second harmonic in the lower branch. The bandwidth of the signals is mainly defined by the burst length. For example, for a 3 MHz signal with 12 cycles burst length, the bandwidth after down-conversion will be for approximately 3/24 MHz, which is appropriately less than the 250 kHz low pass filter suggested in the design. Even for cases when the returned signal would require larger bandwidths, the LPF would just cut the average power in a predictable manner and accurate estimates of the power of the fundamental and second harmonic signals would be possible. (Note that we are interested not in the spectrum shape but in its power.) The above design assumes that we will need both fundamental and second harmonic signals for quantification, since at this time our theory utilizes the ratio of the two.

As mentioned above, we have reduced significantly the requirements (and thus the cost and fragility) for the A/D system - from sampling rates of up to 50 MHz and 12 bit A/D conversion we can come down to rates of 1 MHz and 8 bit A/D. We also eliminated the FFT and thus eliminated its computational time, space, and uncertainty. However, we will need a total of four A/D converters (but since the cost of a smaller bit converter is less, this should be more than compensated for). We could even reduce this number to two by switching a pair of them from the fundamental harmonic to the second harmonic every burst, so that half of the returned signals are

processed on the fundamental harmonic branch and half on the second. This will double the data acquisition time, however.

The final system is shown in Figure 3. This one is a Doppler system that is capable of providing information regarding the contrast agent *flow* in addition to its fundamental and second harmonic backscatter and attenuation characteristics. Its implementation is simpler in that the A/D conversion is done at very low speed (on the order of kHz, compared to 1 MHz for the second approach and 50 MHz for the first approach) and only 8 bits are necessary. Also, if desired, it would be simple to piggy-back it onto the second system if desired. However, Doppler detection of low velocity flows is still not definitively proven (although use of the second harmonic should circumvent several of the problems associated with it).

In Figure 2, the points labelled (A) and (B) are shown as start points for the design in Figure 3. All of the fundamental harmonic received signal processing (the upper two mixers) can be eliminated if we design the system only for Doppler. Also the high speed A/D can be removed from the design, replaced by much lower speed A/D converters. Note that this design is also a quadrature design, and, as a Doppler system, provide information regarding approaching and receding flow. If no directionality is needed, the design becomes that much simpler; only branch A and no 90 degree phase shift is needed. Also, only one A/D is necessary.

III. EXPERIMENTAL METHODS

III.1. Equipment

The components which constituted the system varied according to the system configuration under test for an experiment. The description of the components and the function(s) provided by each follows:

LeCroy 9410 oscilloscope: 4-trace, 150 MHz DSO. The waveform function option provided real time FFT (amplitude and power) as well as averaging, among others. User-controlled cursors allowed accurate and repeatable measurements directly from the 'scope display. An external trigger input provided capability to synchronize the sweep to "difficult" signals.

Hewlett-Packard 8116A function generator: 50 MHz, programmable function. The 8116A provided both continuous-wave (CW) and tone burst capability. Frequency, amplitude, number of cycles, burst repetition rate and other parameters were user-controlled. A gate output provided a TTL-level signal synchronized with the tone burst: the gate rising edge occurred at the start of the burst; the falling edge occurred at time = one-half of the burst repetition interval.

DC power supply: a standard bench supply; triple-output (0 to 6, 0 to -25, 0 to 25).

Preamplifiers: mini-circuits ZFL-500LN and Perry Amplifier 070/40. The preamplifiers were used either singly or cascaded to provide 19, 40, or 70 dB gain.

Transmit/receive switch: fabricated in house. The switch was used in single transducer experiments to isolate the receiver (either a preamplifier or the oscilloscope) from the transmit burst. Isolation was approximately 60 dB; the gate output from the function generator provided the control signal to the switch. The duration in which the transmit signal could pass through the switch to the transducer was adjustable from approximately 2 μs to 1 ms.

Test tank: fabricated in house. This component provided a test environment for the bench-top experiments involving equipment verification, contrast agent characterization and preliminary feasibility information regarding the various system configurations and contrast agent preparations. The tank held two transducers at a 90 degree included angle; contained volume approximately equaled 70 ml. Material: Plexiglas and PVC fittings.

Transducers: Panametrics V323, 2.25 MHz; V384, 3.5 MHz; V310, 5.0 MHz; V312, 10.0 MHz 0.25-in. element, unfocused immersion; V313, 15 MHz 0.25-in. element, spherical focus (0.75-in. focus) immersion transducers.

Contrast agent: Schering AG, SH U 508a (also known by the trade name Levovist), a preparation consisting of granules of galactose and trace palmitic acid, which is prepared for its labelled use by mixing a given quantity of the dry portion with a solvent, either water, saline, or buffer solution.

Tyrode buffer solution: buffer used in contrast agent preparations for *in vitro* experiments (8 g NaCl, 1 g $NaHCO_3$, 0.0576 g NaH_2PO_4 per L deionized H_2O).

As indicated above, discussion with the technical administrator for the grant offered further understanding of the relation of this project to the umbrella project of the Soldier Individual Computer system with medical diagnostic capability. This brought with it the realization that we need not consider display and storage systems and need only supply a front-end system: signal conditioning for the sensor(s) and signal processing which would provide a calibrated output directly related to blood flow in the region of tissue under measurement. The components listed above (along with a desktop PC) served these functions in this proof-of-concept stage.

III.2. Description of Experiments

In general, the goal of the experiments was twofold. One, to explore the limits of usefulness of the experimental parameters of contrast agent concentration, drive voltage, incident frequency, and tone burst length (where appropriate). This was determined by measuring the fundamental and second harmonic responses as well as the mathematically derived ratio of the two. Once these limits were determined, then we proceeded to the second goal, which was to verify the results in a realistic ex vivo preparation, where real animal tissues added another level of complexity to the apparatus, contributing further to attenuation and nonlinear signal generation.

III.2.1. Contrast agent lifetime

In order to have confidence that recorded data reflected activity of controlled parameters and not from unknown behavior of the contrast agent preparation, experiments which explored the time dependent characteristics of the contrast agent in solution were performed. These experiments provided information which allowed us to determine how long an individual test trial could be, in subsequent experiments, before the contrast agent degradation significantly affected the results.

The general equipment configuration is shown in Figures 4 and 5. Figure 4 depicts the connections used in a two transducer tone burst setup; Figure 5 shows the setup used for one transducer. A continuous wave configuration was also used and differed only slightly from that shown in Figure 4 in that the transmit transducer was driven with a continuous sinusoidal voltage.

Two transducers were installed in the test tank. Figure 6 illustrates the holding fixture for a transducer. The transducers were friction-fitted with a rubber cone washer which was sized for a friction fit in the bore of the holding fixture. The insertion collar was sized to be nearly an interference fit with both the bore of the holding fixture and the body of the transducer, but to still allow easy insertion and withdrawal. Use of the insertion collar ensured axial alignment between the transducer and the holding fixture and the fixture arrangement allowed a repeatable fixation of path length.

Prior to transducer insertion, the bore of the holding fixture was filled with a coupling medium (degassed, distilled water). Coupling fluid displaced during transducer insertion simply drained from the relief port in the holding fixture. Provision for a relief port was necessary because of the plastic film membrane which was used early in the project to separate the coupling medium from the solution under experiment in the test tank. A piece of the film was affixed to the end of the holding fixture with rubber cement; after sufficient curing time, mild heat applied to the film shrank it enough to create a taut, wrinkle-free septum. In later experiments we eliminated the coupling medium and the membrane to allow direct contact of the transducer with the test solution.

The transducer mounting fixtures ensured perpendicular alignment of the acoustic axes to avoid direct impingement of the fundamental frequency energy from the transmit transducer onto the receive transducer. Acoustic reflections from bubbly solutions such as the contrast agent occur diffusely (in all directions), so there is no detriment to receiving echoes from a perpendicular angle to the transmitted energy. Second harmonic signals would be observed from a region in the test solution defined by the intersection of the transducer beam patterns. Various concentrations of the contrast agent in Tyrode buffer solution constituted the test solutions used in the tank.

Transducer pairs, in the two transducer configuration, always differed in center frequency; the lower frequency transducer being the transmitter and the higher frequency transducer acted as the receiver. The center frequencies and response characteristics of the transducers and function

generator drive frequencies were chosen to minimize direct second harmonic energy from the transmitter and sensitivity of the receiver to the fundamental frequency energy. This arrangement lent assurance that second harmonic energy was due primarily to the contrast agent nonlinearity, and that the dynamic range of the acquired signals would not tax the acquisition equipment.

The HP function generator supplied the drive voltage for the transmit transducer. In the tone burst configuration, the function generator gate output signal provided oscilloscope sweep synchronization to the transmit signal, which was monitored in tone burst setup on the oscilloscope. Continuous wave configurations, of course, did not require sweep synchronization.

Preamplifiers provided the sensitivity needed by the system to acquire the low level (on the order of tens of microvolts, in some experiments) received signals. Use of the two available preamplifiers allowed a selection of gains determined by which preamplifier was used singly, or by cascading the two preamplifiers. The bench top DC power supply provided operating voltages required by the preamplifier. The amplified receive signal passed on to the oscilloscope.

The waveform functions available in the oscilloscope allowed monitoring of the time domain signal as well as acquisition of a processed signal from which the data were taken. The built in cursor functions provided a means of obtaining accurate readings in a repeatable manner

An experimental trial consisted of acquiring data for a given length of time for a particular set of parameters . A test solution was prepared by weighing the desired amount of dry agent using a precision microbalance (Sartorius) and mixing this by gentle agitation with Tyrode solution (described above). The mixture was gently stirred until no granules were visible and then slowly poured from the beaker into the test tank. To avoid reading the initial highly kinetic transient activity of freshly mixed agent, the newly prepared solution was left undisturbed for some minutes (5 to 10, depending upon the test solution concentration) before measurements in a new trial were started.

The oscilloscope was configured to acquire the received signal and, from this signal, to generate a real time FFT and an average of the FFT over many sweeps (usually 100). The data of interest were the amplitude peaks of the fundamental and second harmonic frequencies as read via the cursors from the averaged FFT. The data were tabulated for serial averages over the duration of the run to record the change in the amplitude peaks as a function of time.

A timer, reset with the initiation of each average, ensured that the data were read from equal intervals of time; the intervals, obviously, were longer than the time required by the oscilloscope to complete, say, a 100 sweep average plus the time needed to read the data from the display (two minute intervals were generally used); the run duration was usually 60 minutes.

III.2.2. Contrast agent second harmonic characteristics

This set of experiments was similar in method to that described in the preceding section. Conceptually the major difference was that, whereas in the previous set of experiments the characteristic under study was strictly amplitude-versus-time, this set of experiments sought to define the contrast agent behavior (represented by second harmonic and fundamental frequency amplitudes; more particularly, the ratio of these amplitudes) as a function of transmit signal amplitude, transmit frequency, contrast agent concentration and tone burst length. The results of the previous experiments guided our choice of the length of the data runs in this set such that time was not a significant parameter.

The amplitude ratio characteristic of the contrast agent may be perceived as occupying a region defined by a hypercube whose axes are the parameters given above. Little work has been published regarding the characteristics of this contrast agent; its behavior, in this context, was very poorly understood. Thus it became essential for us to determine the practical boundaries of the hypercube

The experimental set ups consisted of both the two transducer configuration described previously (and shown in figure 1) and the single transducer set up of figure 2, which will be described in more detail here.

One transducer was installed in the test tank. The test tank could be configured as in the previous section; collected data would represent only the reflection/scattering of second harmonic energy derived from fundamental frequency energy impinging axially on the contrast agent microbubbles during a tone burst (the single transducer configuration implies the use of a tone burst drive). Targets could also be installed in the transducer beam to provide additional data regarding ranging and the effect of interfacial surfaces.

The active (transmit/receive) transducer was connected to the common RF port of a SPDT transmit/receive switch. One throw of the switch connected with the function generator output; the other throw connected to the oscilloscope (either with or without intervening preamplification). The function generator gate output signal provided switching control synchronized to the tone burst output.

Sets of experiments were categorized by the parameter under investigation (e.g., one set of experiments consisted of runs in which only the transmit drive voltage was varied, all other parameters held fixed). Therefore, data were collected for "drive voltage" experiments, "frequency" experiments, "concentration" experiments and "tone burst length" (i.e., the number of cycles in the tone burst) experiments.

Since these data trials were much shorter than those in the lifetime experiments, a set of trials could be completed before the test solution required renewal. Thus, for a given concentration, a trial spanning a drive voltage interval of interest could be repeated over a span of frequencies, generating a two-dimensional data matrix. Data point span and intervals were

predetermined (e.g., 3 to 9 volts of drive in intervals of 0.5 volt) and the amplitude information was again read via the cursors from the averaged FFT waveform.

III.2.3. Contrast agent shadowing characteristics

In addition to the reflection, scattering and nonlinear transformation characteristics addressed by the previous experiments, the contrast agent exhibited an attenuation or absorption characteristic which is commonly known as "shadowing". The effect of shadowing was to reduce the returned signal by up to 100%, depending on the environment. The effect was noticeable when targets were used and when they were not used (in effect, the contrast agent shadowed itself). The mechanism causing this effect is well known and related to the bubbly nature of the agent; bubble are highly efficient reflectors of acoustic energy, and, when present in high enough concentration, will obscure all energies distal to the incident beam. Incidental results from other experiments convinced us that it would be worthwhile to attempt characterization of this behavior.

The experimental set up was predominately that illustrated in Figure 5, with targets in the test tank. The characterization was, again, amplitude versus time. The differences from the lifetime experiments were: 1) amplitudes of the averaged real time received signal, not of the averaged FFT were measured; 2) rather than a decay in amplitude with time, we were looking for a decay in shadowing. The aim was to determine the concentration of the contrast agent based on amplitude readings of received signals reflected from axially aligned targets.

An experimental trial consisted of serial amplitude readings, from at least two targets, starting 10 seconds after the introduction of the contrast agent into the tank and continuing until a steady state condition became established. The readings were performed as rapidly as possible, utilizing the oscilloscope's cursors, and noting the time each reading occurred.

III.2.4. *Ex vivo* experiments

Figure 7 illustrates an experimental set up which utilizes a biological preparation, in this case an excised rabbit kidney. The kidney was immersed (after being purged with normal saline injected into the renal artery) into a solution of normal saline (0.9% NaCl). Small bore, flexible tubing was then cannulated to both the renal artery and vein. The venous line lead to another plastic container which served as a venous reservoir to increase the circulating volume to a more physiologic amount (so that the contrast agent injections would experience a more realistic dilution while circulating) and to accommodate volume changes caused by serial agent injections. Another flexible line connected the reservoir to the inlet port of the circulating pump. The bellows pump head provided a rough approximation of a pulsatile outflow through the flexible plastic tubing cannulated to the renal artery. On the tubing, between the pump outlet and the renal artery, was installed an injection port, to which was attached a three-way stopcock. On the remaining two

ports of the stopcock were attached syringes which contained contrast medium and a saline flush solution.

The contrast agent was prepared by diluting a weighed amount of the granules (generally between 300 and 900 mg) with a small volume of normal saline, in a glass vial to achieve the desired concentration (generally 150 to 450 mg/ml). The solution was then withdrawn into a syringe and attached to the stopcock in preparation for injection. The contrast medium was injected as a bolus, followed by a small bolus injection of flush solution.

The transducer, supported on the arm of a micromanipulator assembly (not shown) had been positioned over the target region of the kidney before contrast injection; the electronics set up was similar to that of Figure 5. Data acquisition began with the completion of the flush injection and continued until the signal amplitude decreased, because of dilution, to the noise floor, or until a steady-state response was noted. Again, amplitude peaks were read via the display cursors from either the averaged FFT (for second harmonic studies) or from the averaged real time received signal (for shadowing studies).

IV. EXPERIMENTAL RESULTS

IV.1. Lifetime experiments

The lifetime data were to provide information we believed would illuminate such properties of the contrast agent as related to subsequent experimental protocols. We wanted to know how the agent changed with time, how repeatable the data from a given concentration would be, how handling might affect the agent's properties and generally how the diluted agent behaved in contact with the experimental environment.

Figure 8 is a graph of a data set typical of this group of experiments. The amplitude (in mV) vs. time (in minutes) behavior of the fundamental frequency peak, the second harmonic frequency peak and the ratio (second/fundamental) are plotted. Characteristic of this group of experiments was the relatively constant value of the amplitude peak ratios during a trial. For the trial depicted in Figure 8 the average ratio was 14.3% with a standard deviation of 2.35%. The ratio exhibited a slight positive correlation with time (average ratio 13.92% during the first 20 minutes of the run; 14.6% during the last 20 minutes) while the standard deviation of the ratio presented with a slightly negative correlation (2.73% in the first 20 minutes; 2.02% for the last 20). The data bore out our subjective impression of a high degree of kinetic activity in a newly mixed solution, which decreases with time. Stirring the test solution during the course of a run seemed to produce a subtle effect on the ratio (inferring, of course, an effect on the fundamental and second harmonic amplitude peaks), as shown in Figure 9. Concentration had little effect on the characteristic profile of the time-dependent behavior.

During this series of experiments, we also found that the plastic film septum (a technique carried over from earlier work) used on the transducer holding fixtures was unnecessary in the configuration employed in the *in vitro* experiments of this project. Removal of the film also had the salutary effect of increasing the sensitivities of the acoustic elements of the system.

IV.2. Second harmonic experiments

We expected this group of experiments to provide the information needed to determine which portion (or portions) of the hypercube were most suitable for this project. Much of the effort in these experiments went toward exploring the extremes of the parameters of interest, i.e., the corners and edges of the hypercube. Correspondingly, drive levels over a range of 200 mV (for CW) to 30 V (for tone burst), concentrations of 0.25 mg/ml to 5 mg/ml, burst lengths of 2 to 12 cycles and frequencies of 1.5 to 3 MHz were utilized.

Figure 10 is a graph of representative data from this family of experiments. The graph depicts the behavior of the second harmonic/fundamental peak amplitude ratio as a function of transmit drive voltage with the tone burst length as a parameter. The contrast agent concentration was 1 mg/ml and the drive frequency was 2.5 MHz. Each data point was obtained from the averaged FFT trace on the oscilloscope, an averaged trace consisting of 250 sweeps. The experimental set up was that of Figure 4.

The amplitudes of the fundamental and the second harmonic generally shifted upward, at a given drive level, as the tone burst length increased (see Figures 10a, b, c, d) and the ratio shifted down. Although gross trends in the curves could be related (e.g., both the fundamental and second harmonic amplitudes roughly increased with drive voltage, at a given tone burst length) from one run to the other, it is clear that details of the curves are significantly variable. Only one of the curves is monotonic.

Not unexpectedly, we found that CW experiments required a lower transmit drive amplitude than tone burst experiments and tolerated a lower contrast concentration while still providing useful data (i.e., the frequency peaks were easily distinguished from the FFT noise floor).

IV.3. Shadowing experiments

Figure 11 is a plot of a screen dump from the LeCroy oscilloscope (to an HP 7470 plotter). The experimental set up was that depicted in figure 1 with the addition of the targets shown in Figure 5. The top trace in Figure 11 is the receive signal; the echoes from each target are easily distinguished. Though the second echo has traversed a greater path length, the target which caused that echo presented a better reflecting surface than did the nearer target; thus the greater amplitude

in the echo from the farther target. The origin of the third echo was probably due to reflection of a high amplitude signal from the walls of the test chamber.

Averaging the receive signal over 50 sweeps produced the bottom trace; the baseline acoustic and electronic noise is significantly reduced. Averaging also minimized the effects of the slight amplitude jitter present on the receive signal. The step displacements in the trace 2 baseline are an artifact of the oscilloscope.

Asymmetry of the echo waveforms about the baseline precluded reading simply the peak values of each echo. Maximum and minimum amplitudes (which provided the peak-to-peak amplitude) for each target echo were read via the cursors.

Figure 12 is a graph of representative data from this series of experiments (note the change in time interval for the last two data points). The salient feature of this data plot is the difference in attenuation (due to the difference in path length) of the return echoes from targets 1 and 2. The theoretical development (see appendix) for utilizing the shadowing characteristic required that attenuation be a function of path length; these experiments verified the theoretical treatment.

IV.4. *Ex vivo* experiments

The bench top *in vitro* experiments provided practical experience with the contrast agent. To better approximate the intended environment for the application, however, experiments utilizing a biological preparation were important to assess the validity of applying *in vitro* results to our conclusions regarding the feasibility of the proposed technique.

Attempts to elicit a second harmonic response were equivocal in this set of experiments. We were unable to record any reliably quantifiable second harmonic data. Given past experience with the agent in Doppler experiments, we propose that this was due to the insensitivity of our transducer system with regard to the second harmonic in a highly scattering, biologic environment. (We did attempt to obtain a more sensitive probe; time limitations, however, made it impossible to integrate it and test it in the system before the end of the Phase I effort.)

The shadowing phenomenon was relatively easy to explore with the rabbit kidney, however. Figure 13 is a graph of the two trials in which we specifically investigated the attenuation characteristic of the contrast agent. The trials were separated by about 15 minutes, and demonstrate encouraging repeatability. The data from trial #2 presents a generally flatter profile with slightly less attenuation. In both trials, steady state conditions occurred approximately 2 minutes after injection. The dips in the curves, we believe, result from recirculation of the contrast agent. The agent possesses a long half life and the background level contributed from trial #1 explains the previously noted characteristic of the trial #2 curve.

Figure 14 is a graph of a trial which is representative of a series performed during a subsequent experiment (in this case, the ordinate is attenuation rather than amplitude). Again,

steady state occurs at approximately 2 minutes post-injection, the effect of residual agent from preceding injections is evident during serial trials, recirculation is variably evident from run to run and the general profile of the attenuation vs. time behavior of the contrast agent is very similar among the trials.

Several of the trials performed during this group of experiments explored the effects of concentration. As anticipated, attenuation displayed a positive correlation to concentration of the injectate. Figure 15 depicts the results of an *in vitro* experiment to also determine the effect of contrast agent concentration on shadowing. The curves resulting from the concentration runs are easily distinguished from each other.

V. CONCLUSIONS

All objectives from the proposal have been met. Additional comments regarding the Soldier Individual Computer program and results from experiments conducted during this project suggest the form of future work.

Foremost is the question of appropriateness of this technique relative to the Soldier Individual Computer project. The methods under consideration here (second harmonic and shadowing) require injection of a contrast agent. Although this precludes the possibility of continuous monitoring of soldier health, conceivably a baseline data could be obtained under controlled conditions and stored and used to compare with data from an injury or trauma situation, at which time another injection would be made.

The second harmonic technique has shown significant promise of practical application in this and other works, and with improvements in understanding, technique and technology could develop into a viable clinical approach to quantifiable measurement of blood flow. Thus, future efforts will continue to be directed toward rigorous testing of the agent, especially in *in vivo* conditions. Rapid advances in computing power will obviously aid in development of a device (in this case, a computer chip for the Soldier Individual Computer).

The well known phenomenon of shadowing demonstrates the immediately attractive attributes of predictability and docility. However, until now, this has been viewed as an annoyance to be avoided in ultrasound diagnostics, never studied for practical use. The preliminary work performed here shows much promise for perfusion quantification, and further work will elaborate upon these experiments.

VI. REFERENCES

Burns, S.M. and Reid, M.H., "Design for an ultrasound-based instrument for measurement of tissue blood flow," *Biomat., Art. Cells, Art. Organs 17*, 61-68 (1989).

Burns, P.N., J.E. Powers and T. Fritzsch, "Harmonic Imaging: New Imaging and Doppler Method for Contrast-enhanced US," Proceedings of Radiological Society of North America Fall Meeting 1992, *Radiology*, 142 (October 1992).

Dymling, S.O., Persson, H.W. and Hertz, C.H., "Measurement of blood perfusion in tissue using Doppler ultrasound," *Ultrasound Med. Biol.17*, 433-444 (1991).

Monaghan, M.J., P.J. Quigley, J.M. Metcalfe, S.D. Thomas and D.E. Hewitt, "Digital subtraction contrast echocardiography: a new method for the evaluation of regional myocardial perfusion," *British Heart Journal 59*, 12-19 (1988).

Ong, K., G. Maurer, S. Feinstein, W. Zwehl, S. Meerbaum and E. Corday, "Computer methods for myocardial contrast two-dimensional echocardiography," *J. of the Am. Coll. of Cardiology 3*, 1212-8 (1984).

Saumet, J.L., A. Dittmar and G. Leftheriotis, "Non-invasive measurement of skin blood flow: comparison between plethysmography, laser-doppler flowmeter and heat thermal clearance method," *Int J. Microcirc: Clin Exp 5*, 73-83 (1986).

Schrope, B. and V.L. Newhouse, "Second harmonic ultrasonic blood perfusion measurement," *Ultrasound in Medicine and Biology*, **19**(7), 1993, pp. 567-580.

Schrope, B., Newhouse, V.L. and Uhlendorf, V., "Simulated capillary blood flow measurement using a nonlinear ultrasonic contrast agent," *Ultrasonic Imaging 14*, 134-158 (1992).

Ten Cate, F., K. Drury, S. Meerbaum, J. Noordsy, S. Feinstein, P. Shah and E. Corday, "Myocardial contrast two-dimensional echocardiography: experimental examination at different coronary flow levels," *J. of the Am. Coll. of Cardiology 3*, 1219-26 (1984).

VII. APPENDIX 1: Theoretical Development of Shadowing Phenomenon

In addition, we have serendipitously discovered an interesting phenomenon related to the prominent shadowing effect of the contrast agent. This is a repeatable effect, and seems to have stable behavior. Based on preliminary observations from this effect, we have developed a new theory to utilize this phenomenon for perfusion quantification. This will briefly be described here; a full analysis will of course be presented in the final project report.

Assuming that the backscattered signal from a target located at a distance x from a pulsed system can be described by:

$$r(x) = T\rho G(x)e^{-2\alpha x} \qquad \text{(VII.1)}$$

where r is the received signal, T is the transmitted signal, ρ is the target reflection coefficient, α is a constant attenuation coefficient and G is the transducer pattern envelope function. If we assume that the attenuation coefficient is varying across the medium, equation (VII.1) takes the following form:

$$r(x) = TG(x)\rho e^{-\int 2\alpha(x)dx} \qquad \text{(VII.2)}$$

If we assume that the attenuation coefficient in a small region can be considered constant, we can write the following two equations for the received echoes from the targets. The received echo from the first target would be:

$$r(x_1) = TG(x_1)\rho_1 e^{-\int_0^{x1} 2\alpha(x)dx} \qquad \text{(VII.3)}$$

and from the second target:

$$r(x_2) = TG(x_2)\rho_2 e^{-\int_0^{x2} 2\alpha(x)dx} = TG(x_2)\rho_2 e^{-\int_0^{x1} 2\alpha(x)dx} e^{-\int_{x1}^{x2} 2\alpha(x)dx} = TG(x_2)\rho_2 e^{-2\alpha_x\Delta x - \int_0^{x1} 2\alpha(x)dx} \qquad \text{(VII.4)}$$

where α_x is the "constant" attenuation coefficient between the two targets and Δx is the distance between the targets.

Now, assuming that the marginal attenuation coefficient caused by a perfused contrast agent is directly proportional to the contrast agent density (concentration). Thus, the marginal attenuation coefficient due to the contrast agent will be $\alpha_n = \gamma N$. So, in general, we add the term $\alpha(x)$ to the term $\gamma N(x)$ to estimate the total attenuation coefficient.

Equations (VII.3) and (VII.4) describe the received signal from two closely spaced targets before contrast agent injection. After contrast agent injection and with the added assumption that the contrast agent density between the two targets can be assumed constant, equations (VII.3) and (VII.4) become:

$$r_n(x_1) = TG(x_1)\rho_1 e^{-\int_0^{x1} 2(\gamma N(x) + \alpha(x))dx} \qquad \text{(VII.5)}$$

$$r_n(x_2) = TG(x_2)\rho_2 e^{-2(\alpha_x+\gamma N_x)\Delta x - \int_0^{x1} 2(\gamma N(x) + \alpha(x))dx} \qquad \text{(VII.6)}$$

Denoting the ratio between equation (VII.4) and equation (VII.3) as R and between equations (VII.6) and (VII.5) as R_n we obtain:

$$R = \frac{\rho_2 G(x_2) e^{-2\alpha_x\Delta x}}{\rho_1 G(x_1)} \qquad \text{(VII.7)}$$

$$R = \frac{\rho_2 G(x_2) e^{-2(\alpha_x+\gamma N_x)\Delta x}}{\rho_1 G(x_1)} \qquad \text{(VII.8)}$$

From equations (VII.7) and (VII.8) we can extract N_x:

$$N_x = \frac{Ln\left(\frac{R}{R_n}\right)}{2\gamma\Delta x} \qquad \text{(VII.9)}$$

Equation (VII.9) represents the solution of density of contrast agent, which is presumed is directly proportional to amount of tissue perfused (between the two targets). Further refinement of this

theory to in vivo situations, as well as further experimentation to verify the assumptions, is in progress.

VIII. APPENDIX 2: Theoretical Development of Second Harmonic Quantification

It has been shown in previous analyses that will not be repeated here (Schrope et al, 1992; Schrope and Newhouse, 1993) that ultrasound by itself is unsuitable for detection of microcirculatory blood flow, especially that located in deep tissues. When a specific ultrasound contrast agent (SHU-508 or Levovist®, Schering AG and Berlex Laboratories) is added to the system, however, a unique "signature" is applied to the slow, small signal blood flow that allows it to be unambiguously detected over other noise in the system, including signal from surrounding tissue movements. The contrast agent, consisting of a suspension of microbubbles on the order of two to three microns in diameter, is administered in a small volume (usually less than 5 ml) intravenous bolus. In the present application, the three-step management of critical trauma victims, that is, Airway --> Breathing --> Circulation, dictates that an intravenous line be placed for administration of various medications and fluids as needed. This IV site can also be used to administer the agent necessary for the measurement. Further as yet unpublished work is presented here to describe the efforts at quantification of the data as a measure of blood perfusion.

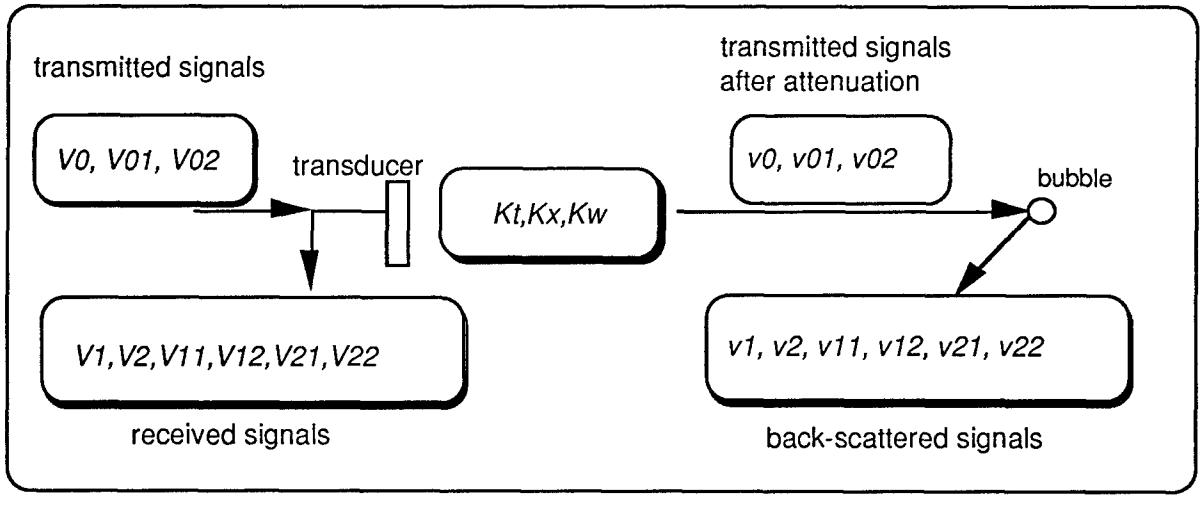

Figure VIII1: Signals and attenuation coefficients used in the following analysis and should be used as a reference block.

Figure VIII1 shows signals and attenuation coefficients used in the following analysis and should be used as a reference block diagram. We assume the first and second harmonic signal voltages (in the analysis, we use voltages and pressures interchangeably) of the backscattered signals near the bubble site can be represented by the following expressions:

$$v_1 = \sigma v_0 \qquad \text{(VIII.1)}$$

$$v_2 = \sigma(a_1 v_0 + a_2 v_0^2) \qquad \text{(VIII.2)}$$

According to eq. (VIII.1), the first harmonic backscattered pressure signal v_1 near the bubble site is directly proportional to the transmitted signal strength near the bubble site multiplied by the scattering cross section of the bubble, σ_1. Likewise, the second harmonic signal is proportional to the bubble scattering cross section multiplied by a second order polynomial expression.

The transmitted signal V_0 is attenuated by frequency dependent attenuation of the tissue which is characterized by the coefficient $K_t(r)$ (for clarity, we omit the dependence on r in the following analysis and assume a set range delay) and by transducer-skin and organ wall interface losses which are represented by the coefficient K_x. The signal strength near the bubble site is also determined by the transducer beam geometry K_w. v_0 can thus be written as:

$$v_0 = V_0 K_{x1} K_{t1} K_{w1} \qquad \text{(VIII.3)}$$

The 1 added to the subscripts denotes that the attenuation and beam geometry coefficients apply to the first harmonic frequency. The signal v_1 (the first harmonic backscattered pressure generated by a single bubble) is according to eq. (VIII.1):

$$v_1 = \sigma V_0 K_{x1} K_{t1} K_{w1} \qquad \text{(VIII.4)}$$

The average backscattered voltage from an ensemble of N randomly distributed bubbles at the receiving transducer is:

$$V_1 = V_0 \sqrt{N} \sigma K_{x1}^2 K_{t1}^2 K_{w1}^2 \qquad \text{(VIII.5)}$$

The backscattered voltage is directly proportional to the square root of the number of bubbles in the range cell (as the received power is directly proportional to N). Reflecting back to the transducer, the backscattered signal is attenuated again by the K_{x1}, K_{t1} and K_{w1} coefficients described above.

For the second harmonic signal for a single bubble (see eq. (VIII.2))

$$v_2 = \sigma(a_1 v_0 + a_2 v_0^2)$$

$$v_2 = \sigma(a_1 V_0 K_{x1} K_{t1} K_{w1} + a_2 V_0^2 K_{x1}^2 K_{t1}^2 K_{w1}^2) \qquad \text{(VIII.6)}$$

and the signal received by the transducer (second harmonic) is:

$$V_2 = v_2 K_{x2} K_{t2} K_{w2} \qquad \text{(VIII.7)}$$

The 2 added to the subscripts denotes that the attenuation and beam geometry coefficients apply to the second harmonic frequency. Note that the attenuation and transducer beam coefficients for the second harmonic signal are different than for the first harmonic signal. The received second harmonic signal is thus determined by both the first harmonic coefficient (transmitted) and the second harmonic coefficients (reflected)

$$V_2 = \sigma(a_1 V_0 K_{x1} K_{t1} K_{w1} + a_2 V_0^2 K_{x1}^2 K_{t1}^2 K_{w1}^2) K_{x2} K_{t2} K_{w2} \qquad \text{(VIII.8)}$$

The received signal from N bubbles is thus:

$$V_2 = V_0 \sqrt{N} \sigma K_{x1} K_{t1} K_{w1} K_{x2} K_{t2} K_{w2} [a_1 + a_2 V_0 K_{x1} K_{t1} K_{w1}] \qquad \text{(VIII.9)}$$

The result of eq. (VIII.9) represents the general expression for the second harmonic received signal from an ensemble of randomly distributed scatterers. We will use this fundamental result in the next section to derive the attenuation expression and then solve for the number N of the scatterers in the range cell.

Attenuation Estimation

The attenuation can be derived from the ratio of the received second harmonic signals for two different transmitted signals, say V_{01}, V_{02}. Denote the received second harmonic signals respectively as V_{21}, V_{22}. We get (from eq. (VIII.9)):

$$\frac{V_{21}}{V_{22}} = \frac{V_{01}[a_1 + a_2 K_{x1} K_{t1} K_{w1} V_{01}]}{V_{02}[a_1 + a_2 K_{x1} K_{t1} K_{w1} V_{02}]} \qquad \text{(VIII.10)}$$

Denote:

$$\beta = K_{x1} K_{t1} K_{w1} \quad \text{(attenuation to bubble - first harmonic)} \qquad \text{(VIII.11)}$$

$$R_0 = \frac{V_{21}}{V_{22}};\ R_1 = \frac{V_{01}}{V_{02}}$$

where V_{21}, V_{22} are the second harmonic received signals generated by the contrast agent due to V_{01}, V_{02} respectively. We get from eq. (VIII.10) and eq. (VIII.11):

$$\frac{R_0}{R_i} = \frac{1 + \frac{a_2}{a_1}\beta V_{01}}{1 + \frac{a_2}{a_1}\beta V_{02}} \qquad \text{(VIII.12)}$$

and

$$\beta = \frac{\frac{a_2}{a_1}\left(\frac{R_0}{R_i} - 1\right)}{V_{01} - \frac{R_0}{R_i} V_{02}} \qquad \text{(VIII.13)}$$

If a_2/a_1 is given, the number of bubbles in the range cell can be extracted using eq. (VIII.5)

$$V_{11} = \sigma V_{01} \sqrt{N} \beta^2$$

where V_{11} is the first harmonic received signal due to the transmitted signal V_{01}.

$$N = \frac{V_{11}^2}{\sigma^2 V_{01}^2 \beta^4} \qquad \text{(VIII.14)}$$

The challenge is to obtain V_{11}, i.e., to subtract the tissue echoes from the received first harmonic signal that contains both the bubbles as well as tissue echoes.

Calibration

In the previous section, we assumed that the ratio a_1/a_2 was known. In some cases this value may not be provided by the contrast agent vendor and it must be evaluated. This can be done in the following manner: in an experiment where N, σ, V_0 and V_1 are known, the attenuation term β can be extracted using eq. (VIII.5)

$$\beta = \sqrt{\frac{V_1}{V_0 \sqrt{N}\,\sigma}} \qquad \text{(VIII.15)}$$

a_1/a_2 can now be calculated using eq. (VIII.15) using two different transmitted signals. In order to improve the accuracy of the quantity β, multiple experiments with a variety of transmitted signal voltages V_0 as well as bubble concentration N should be carried out and averaged. Likewise, to improve the estimate accuracy of the ratio a_1/a_2 several experiments with different transmitted signal voltages should be carried out and averaged. This should also provide a test to the second harmonic signal generation model that assumes that two terms in the polynomial expansion of eq. (VIII.2) are sufficient. If the ratio a_1/a_2 shows a significant trend (instead of just random experimental variations), the model should probably be refined as will be discussed later.

A practical way to calibrate the system can be achieved by mixing a known quantity of the contrast agent with a known quantity of water to create a "standard" to which all other measurements will be related. In this case we first estimate β using eq. (VIII.15). Note that the quantity defined by this "standard" is of $N\sigma^2$, and not only of concentration N. This standard does not have to be a close approximation of the actual quantity of $N\sigma^2$. It can be set arbitrarily to 1, for example. This, naturally, will cause the ratio a_1/a_2 to be tied to this arbitrary "standard". While not affecting the relative quality of concentration estimates, it may cause confusion if a standardized "standard" is not defined.

Microvascular Blood Flow Estimation

In this section we describe the underlying fundamental theory of the proposed innovation. While there have been quite a few attempts in the past to use ultrasound for microcirculatory blood flow estimation, none of the proposed techniques provides adequate solution to the problem (see section c).

The main problem with the current methods is that the transmitted and received signals are attenuated by unknown amount, by highly varying tissue media, blood vessel walls and transducer-skin interface. It is thus impossible to estimate accurately the reflection from the tissue, even though contrast agents for image contrast enhancement are available.

Our breakthrough approach, as was explained earlier, is based on the use of a unique contrast agent, SHU-508 (Schering AG and Berlex Laboratories). However, unlike other approaches using contrast agents, such as area under the curve or half-lifetime (Monaghan et al, 1988; Ong et al, 1984; Ten Cate et al, 1984), our method is based on the nonlinear characteristics of this particular contrast agent. These agents that typically look like spheres produce in many cases relatively strong signals at twice the frequency of the transmitted signal (Schrope et al, 1992; Schrope and Newhouse, 1993; Burns et al, 1993). We refer to these signals as second harmonic signals. In the proposed method, an ultrasonic signal with a given frequency is transmitted

towards the region of interest (which is the region for which we attempt to estimate the microcirculatory blood flow). The contrast agent, due to its nonlinear nature, generates a second harmonic signal which is received by the receiving transducer. The first harmonic signal is also received by a receiving transducer (possibly the same transducer).

The basic idea behind the proposed technique is that the characteristics of the medium, i.e., its attenuation characteristics, can be extracted from the ratio of the received second harmonic signals from two different transmitted signal amplitudes. For example, we transmit first a signal at 10 V and record the received second harmonic signal amplitude from a region of interest, say, 10 mV. We repeat this experiment with a different transmitted signal, say 20 V, and record the received second harmonic signal amplitude for this case, say 30 mV. Note that due to the nonlinear behavior of the contrast agent the second harmonic tripled for only a two-fold increase in the transmitted signal strength. As the following analysis will clearly show, tissue attenuation coefficients can be extracted from the ratio of the two second harmonic signals with respect to the ratio of the transmitted signals (in this case the output ratio is 3 = 30/10, while the input ratio is 2 = 20/10). The main reason that we can estimate the attenuation is due to the fact that the ratio between the two second harmonic signals depends solely on the strength of the transmitted signal at the contrast agent site. The stronger the transmitted signals at the contrast agent site, the larger the second harmonic signal ratio would be. Thus, we can infer from this ratio the signal strength at the contrast agent site and consequently the medium attenuation. In practice, the two different transmitted signals would be transmitted sequentially in a rapid rate, say every 0.5 to 1 msec. This way the spheres that compose the contrast agent do not change significantly their random relative positions and the target can be considered to be unchanged.

Once the attenuation has been quantified, we would "isolate" the echo from the contrast agent and estimate very accurately the concentration of the contrast agent. As was explained earlier, the contrast agent is injected in a controlled fashion. Thus, the concentration of the injected contrast agent is known. As a consequence an accurate estimate of blood perfusion would be possible.

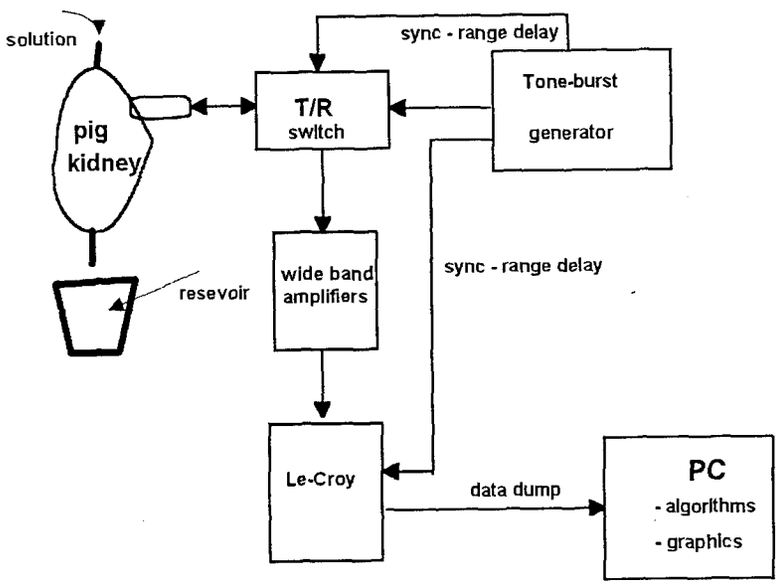

Figure 1: Block diagram of system design number one, based on existing off-the-shelf components.

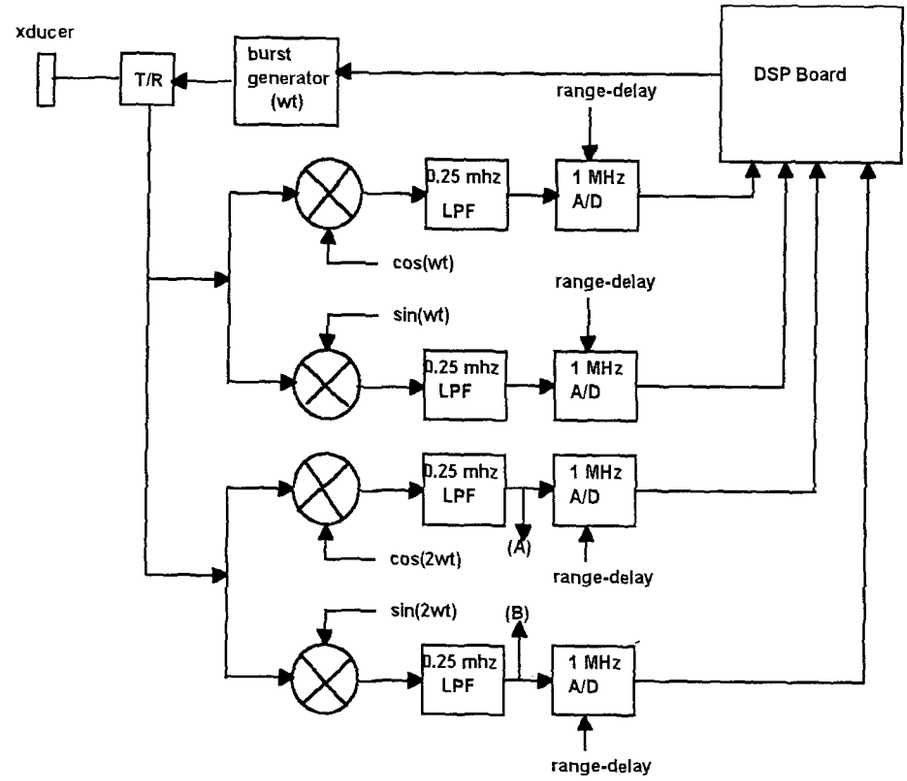

Figure 2: Block diagram of system design number two, where much of the processing has been transformed to DSP.

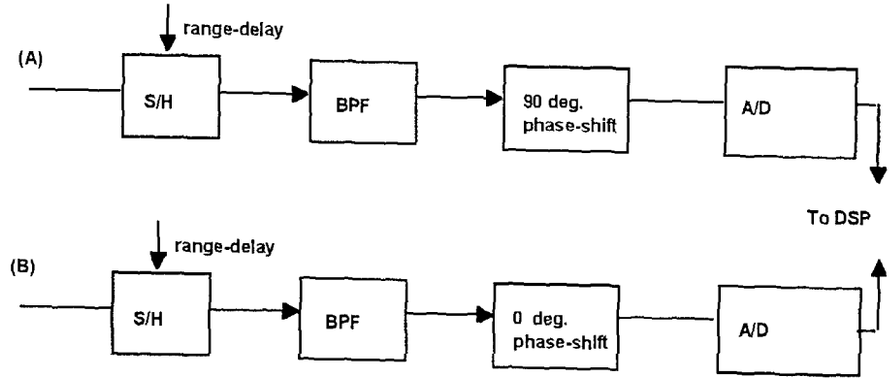

Figure 3: Block diagram of system design number three, with Doppler capability.

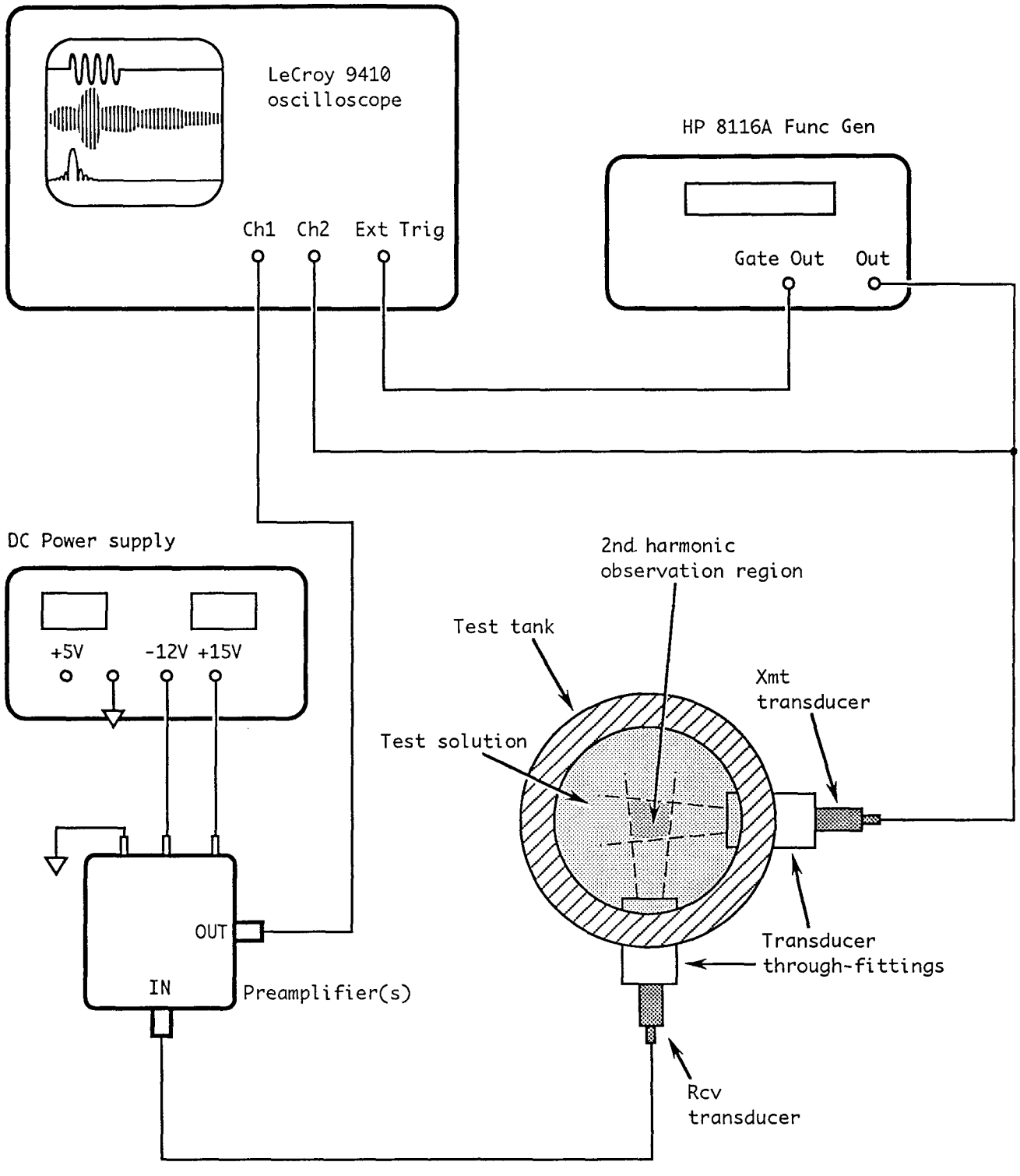

Figure 4: *In vitro* experimental apparatus - two unfocused transducers, tone burst transmitted signal.

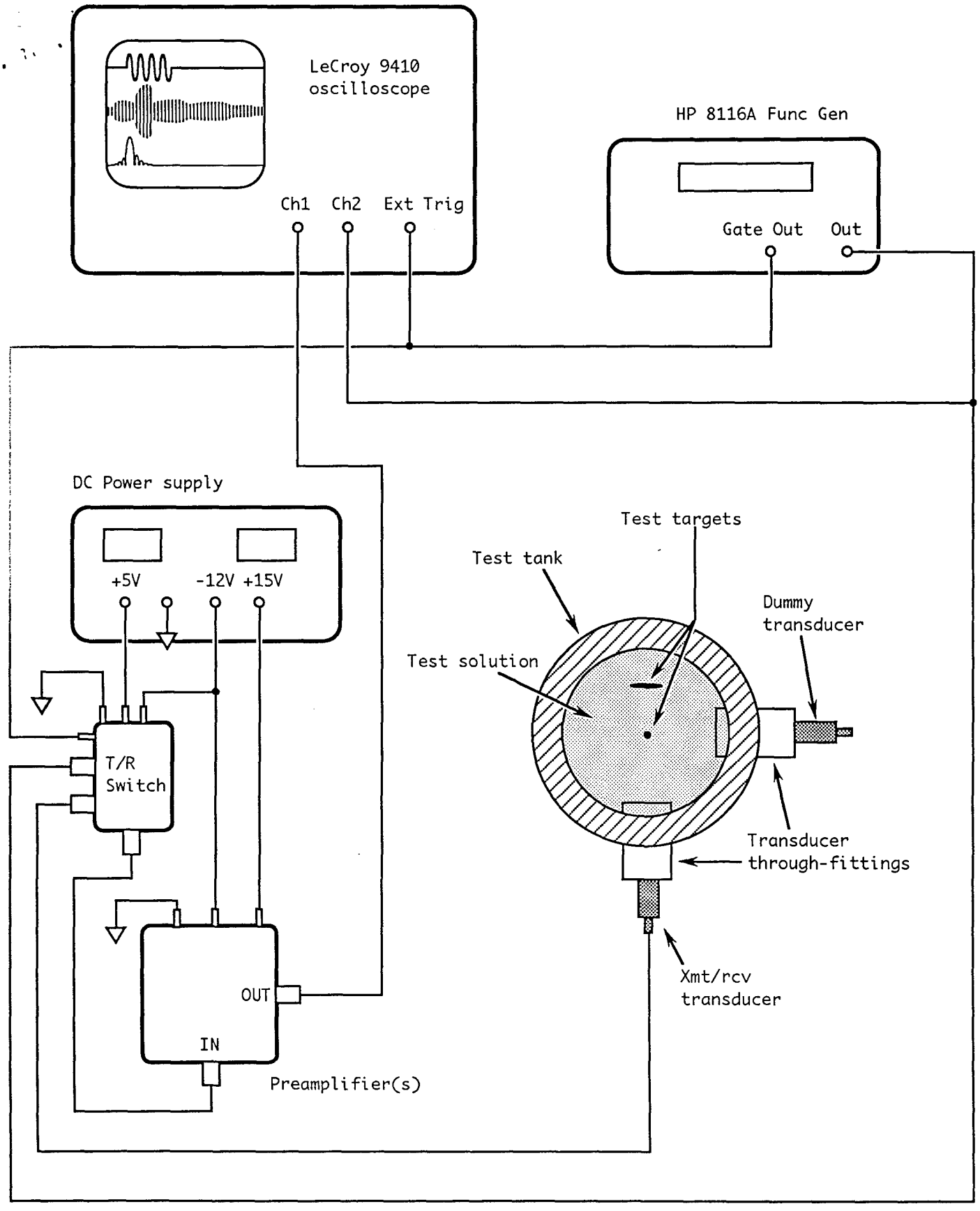

Figure 5: *In vitro* experimental apparatus - single transducer, tone burst transmitted signal.

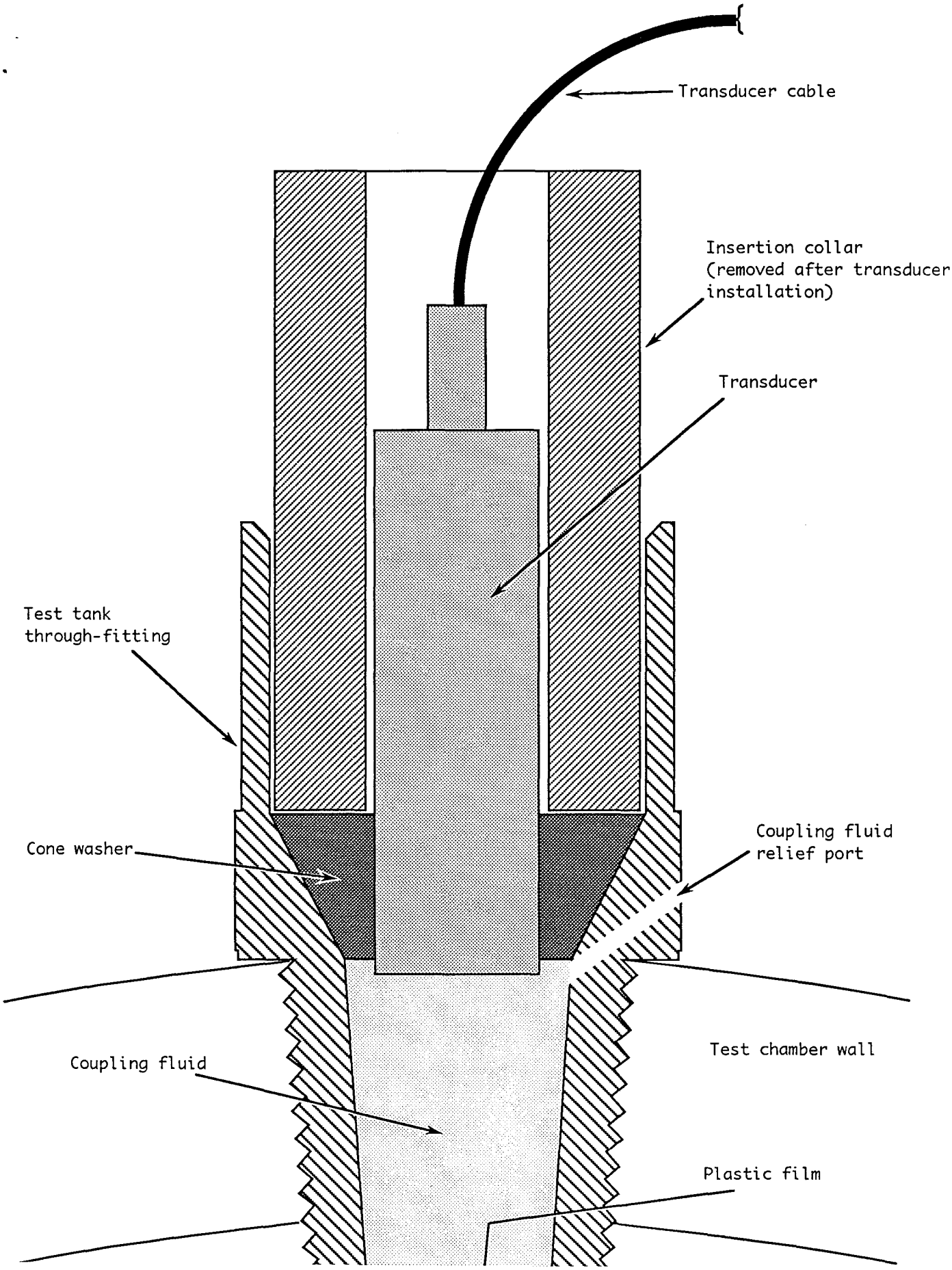

Figure 6: Detail of transducer fitting assembly.

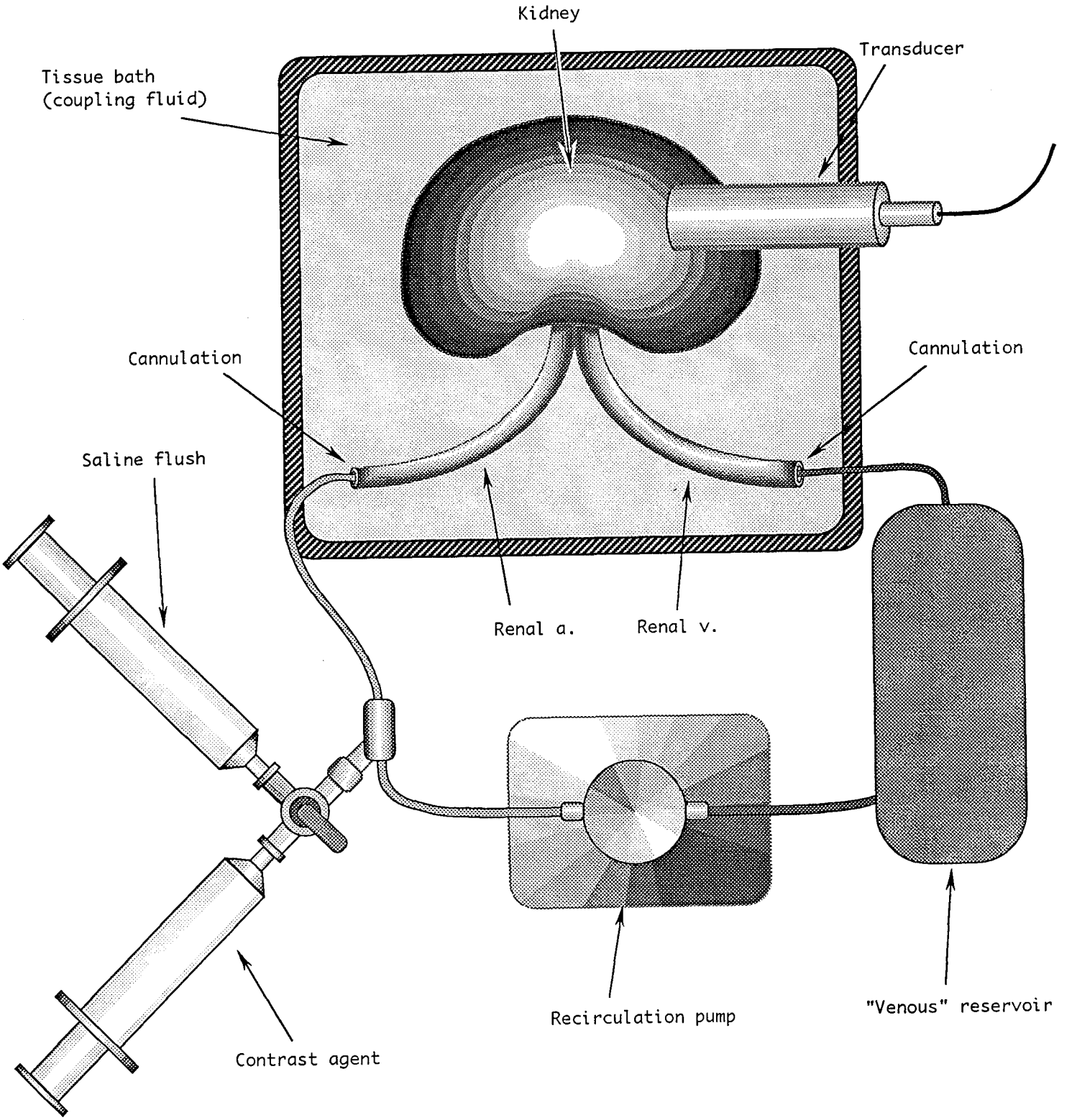

Figure 7: *Ex vivo* experimental preparation, single transducer set up.

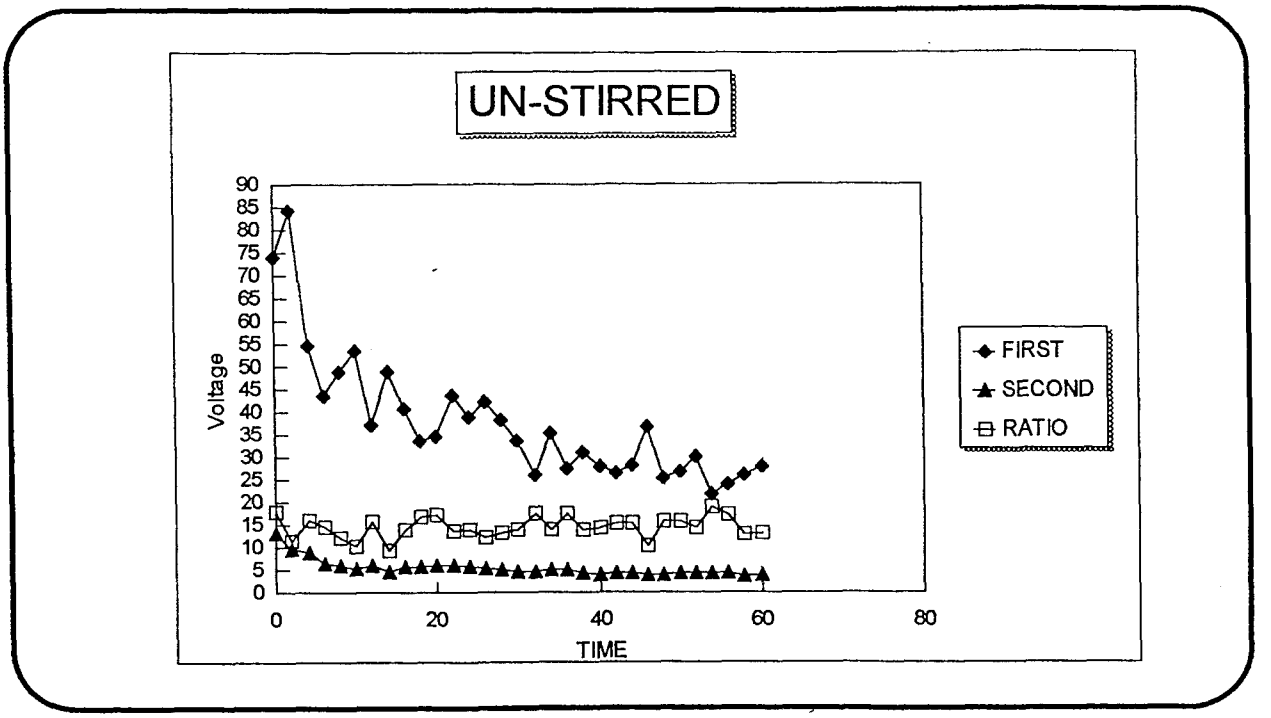

Figure 8: Received signal amplitude versus time for lifetime experiments, unstirred condition.

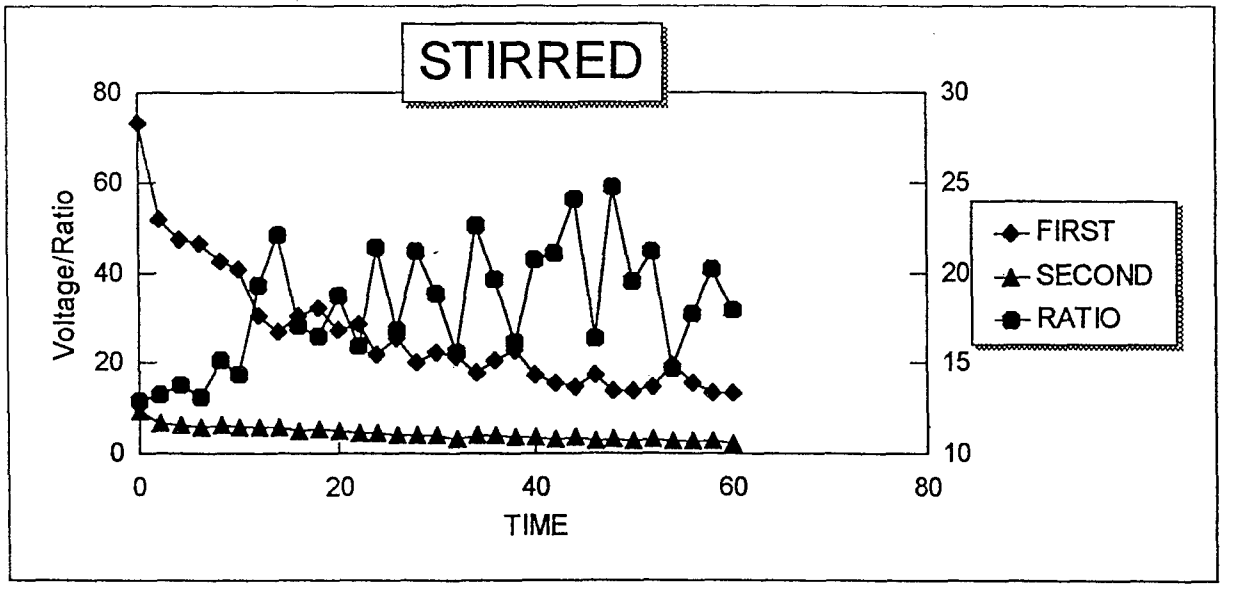

Figure 9: Received signal amplitude versus time for lifetime experiments, stirred condition.

Figure 10: Second harmonic to fundamental amplitude ratio as a function of transmit drive voltage, comparing results for a variety of tone burst lengths (five graphs).

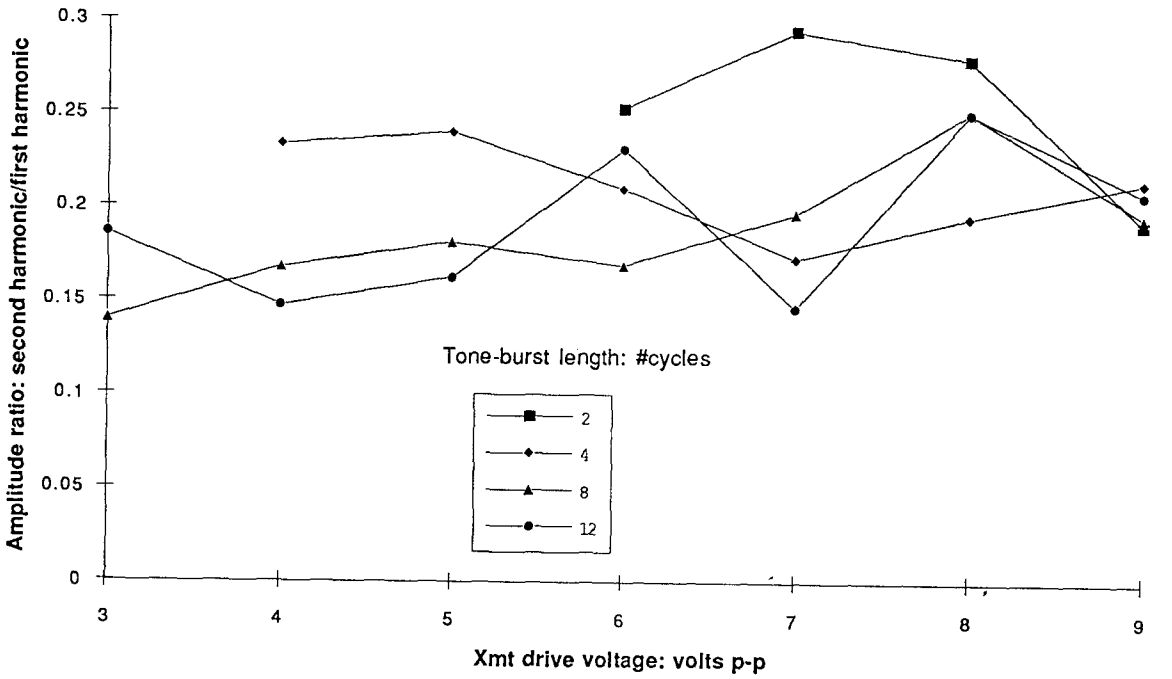

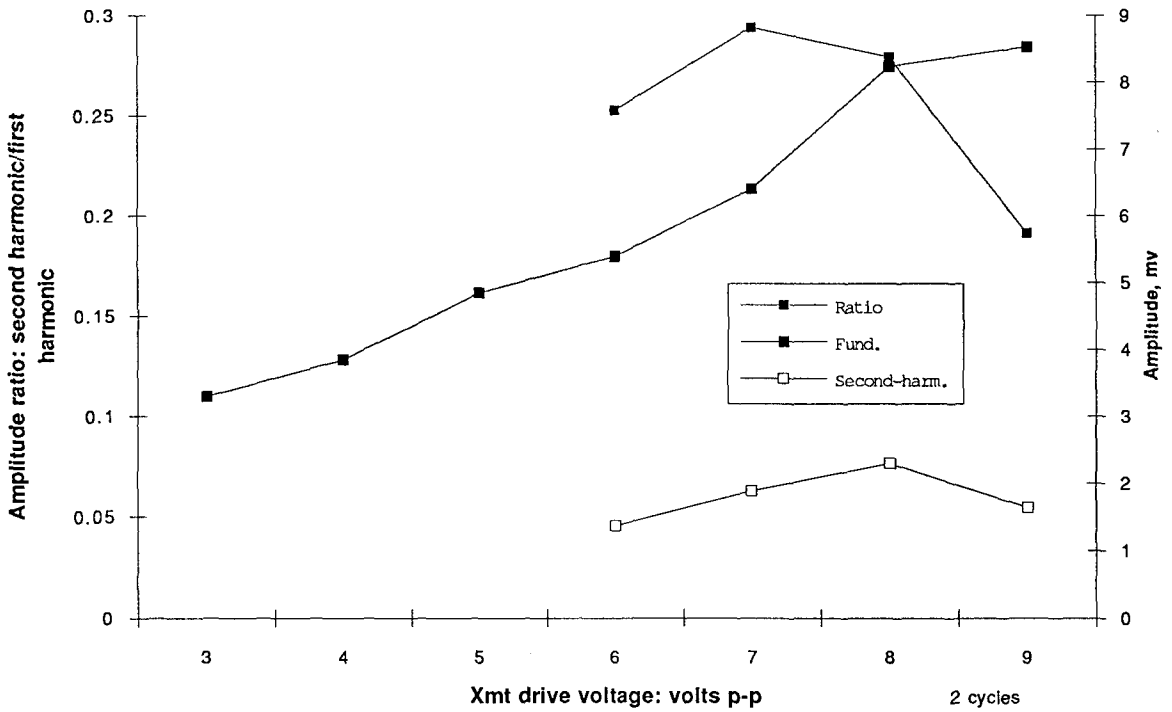

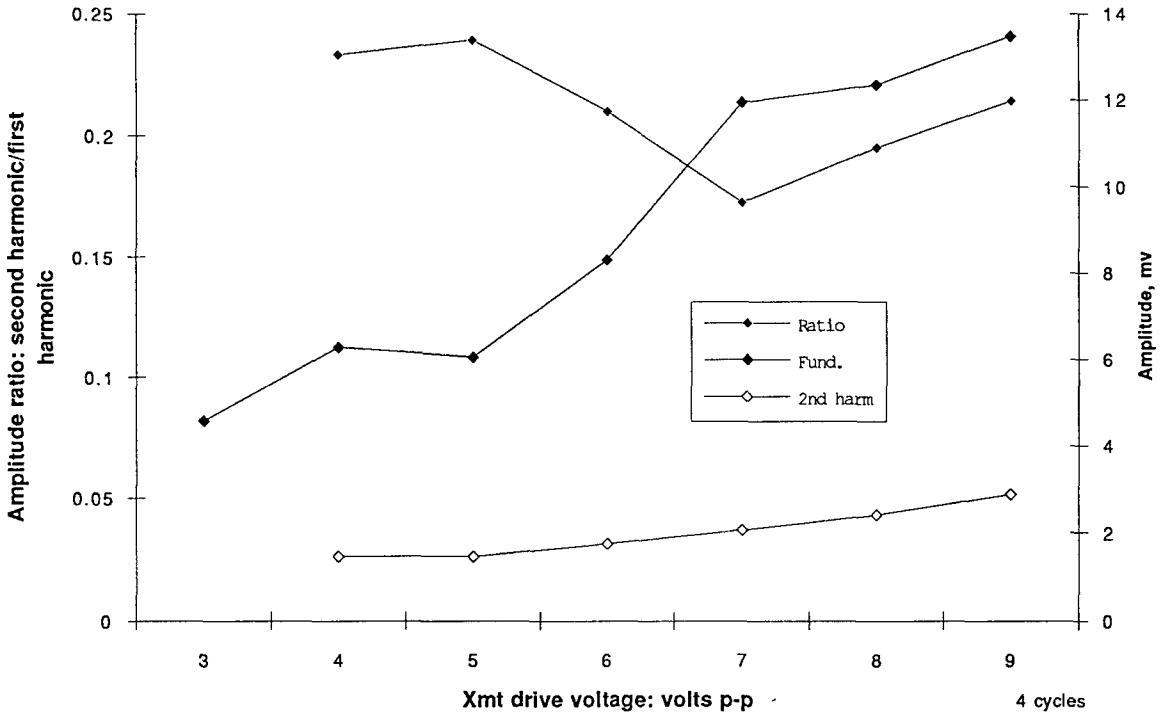
Amplitude ratio: second harmonic/first harmonic
Amplitude, mv
Ratio
Fund.
2nd harm
Xmt drive voltage: volts p-p
4 cycles

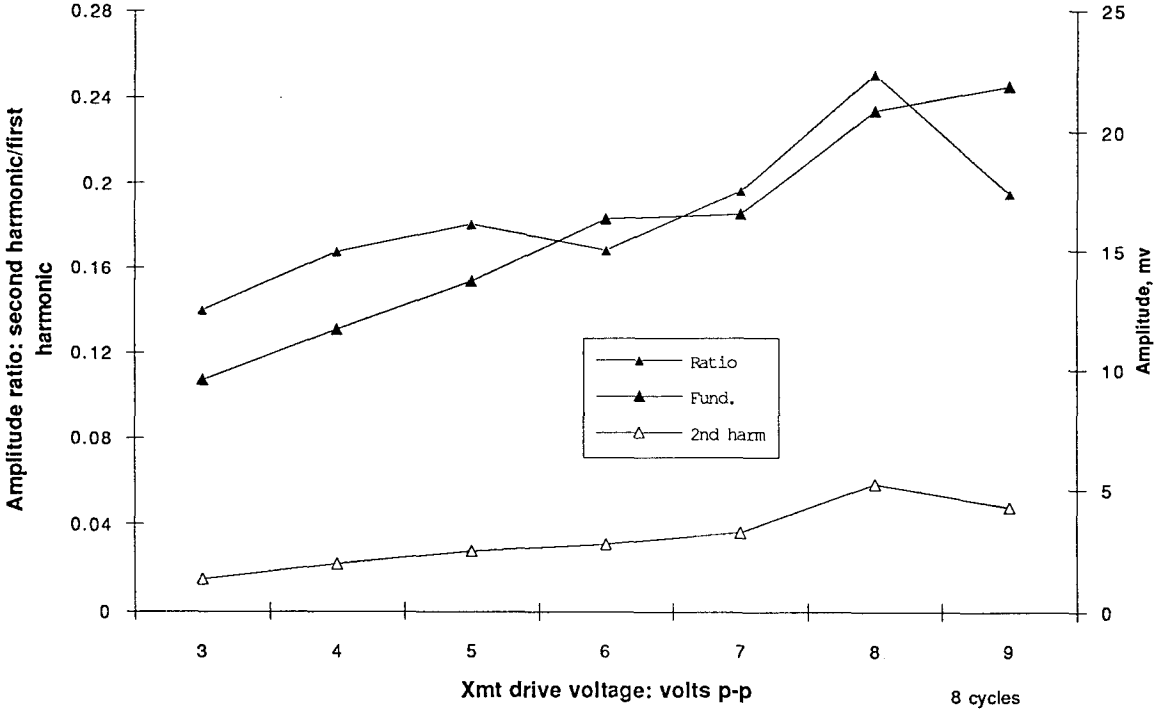
Amplitude ratio: second harmonic/first harmonic
Amplitude, mv
Ratio
Fund.
2nd harm
Xmt drive voltage: volts p-p
8 cycles

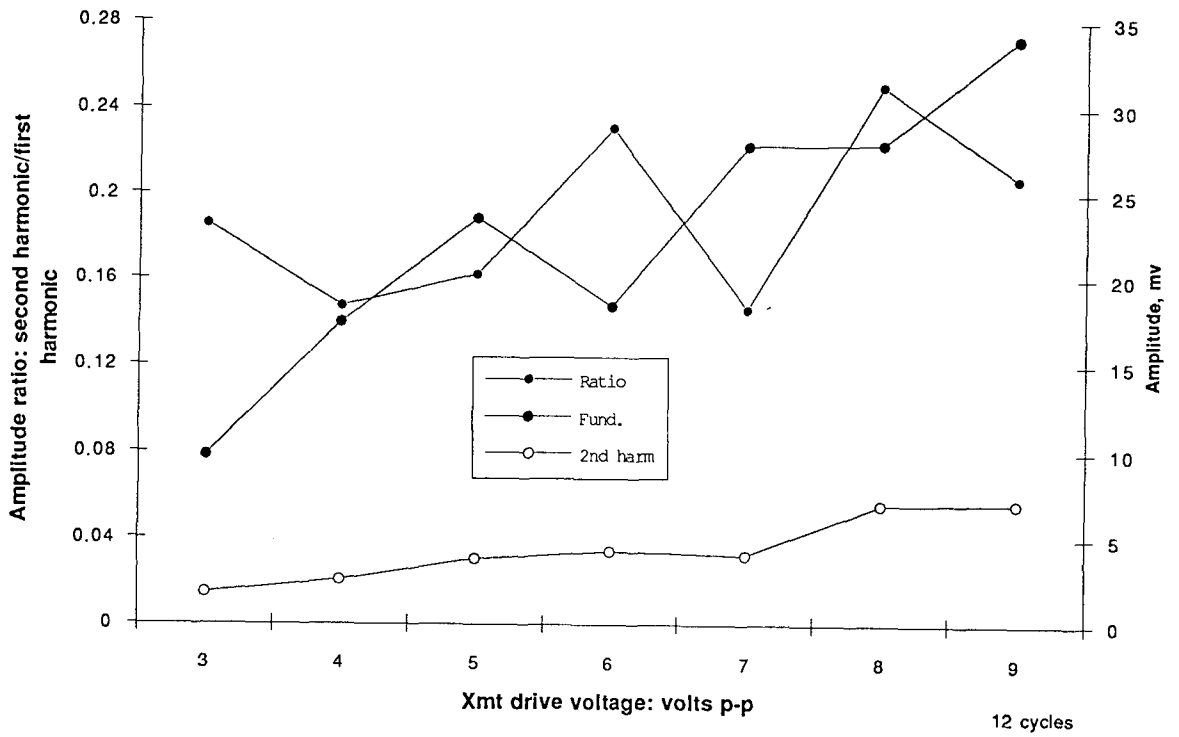
0.28
0.24
0.2
0.16
0.12
0.08
0.04
0
Amplitude ratio: second harmonic/first harmonic
35
30
25
20
15
10
5
0
Amplitude, mv
Ratio
Fund.
2nd harm
3
4
5
6
7
8
9
Xmt drive voltage: volts p-p
12 cycles

P_1 = echo from needle target

P_2 = echo from aluminum strip target

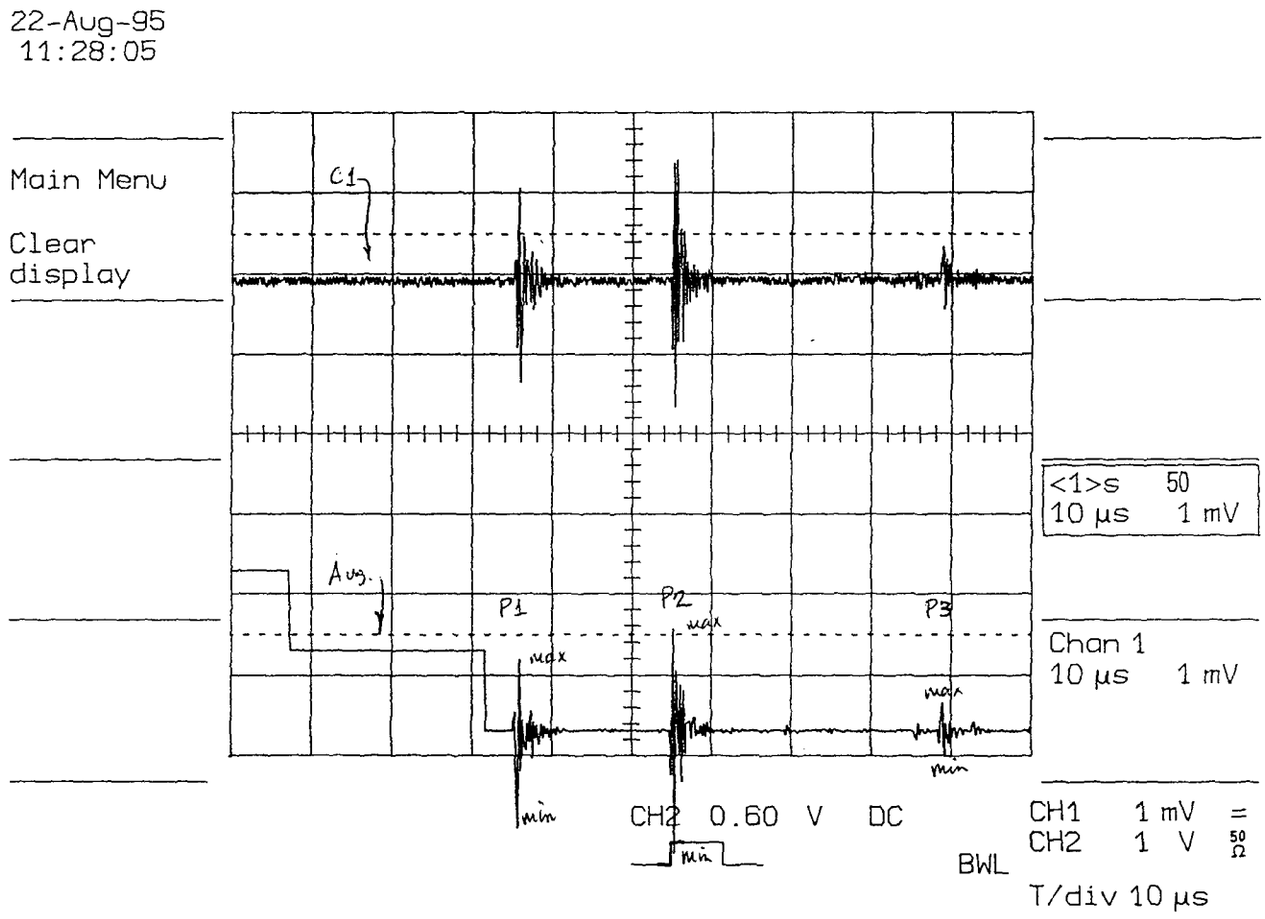

Figure 11: Oscilloscope screen dump of target echoes, shadowing experiment.

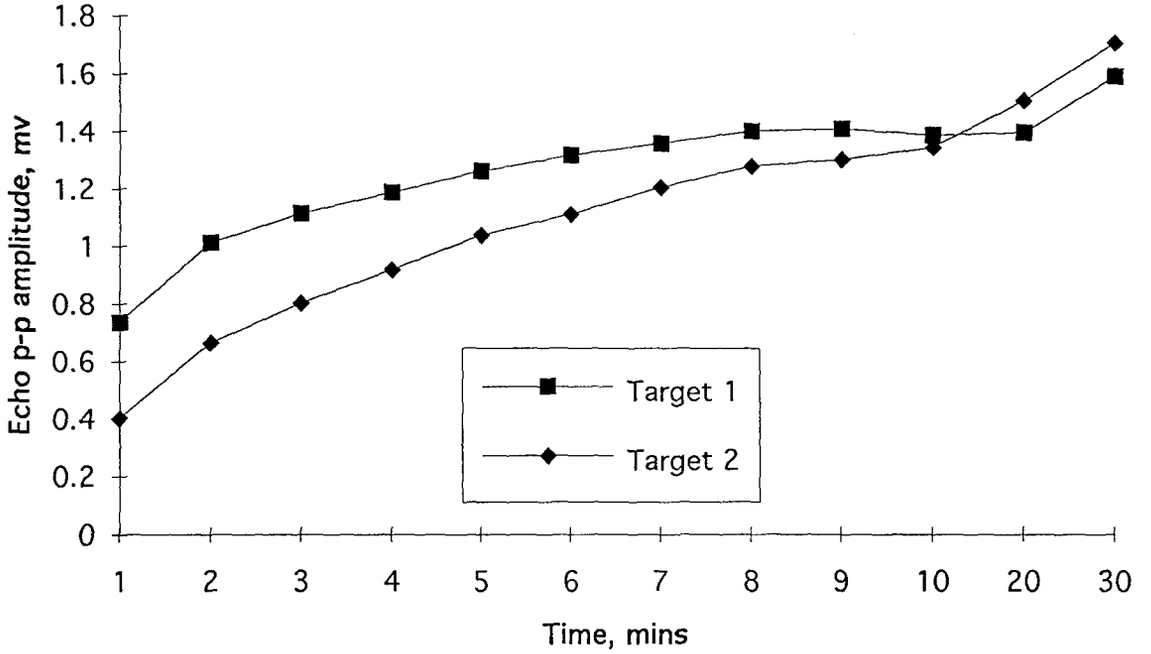

Figure 12: *In vitro* shadowing experiment - concentration of contrast agent = 0.25 mg/ml, transmit frequency = 3.59 MHz, drive voltage = 4.8 volts (peak-to-peak), burst length = 2 cycles; data averaged 50 times.

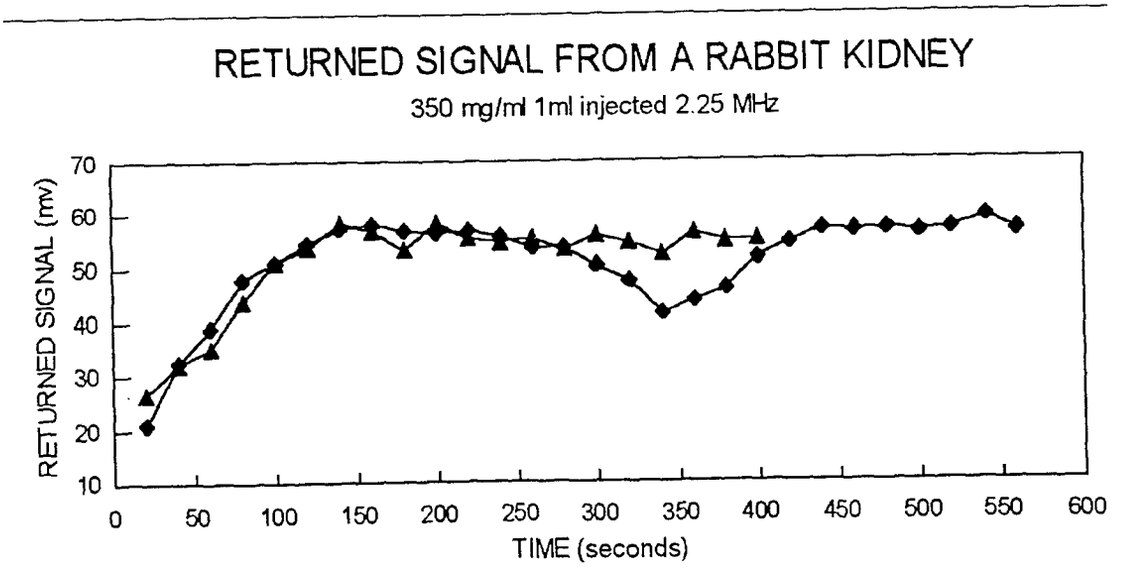

Figure 13: *Ex vivo* shadowing experiment - time-dependent characteristic of raw received signal. The two lines depicted indicate two different trials.

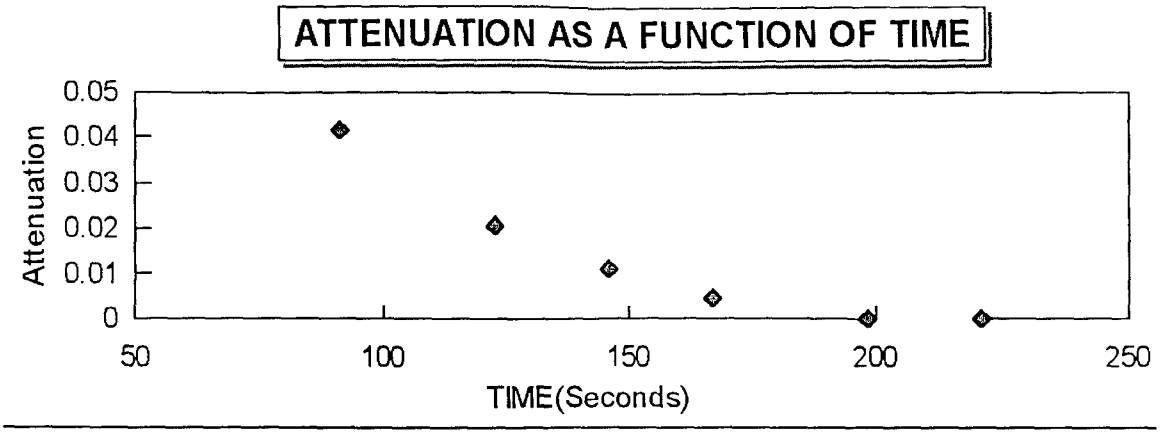

Figure 14: Shadowing (or attenuation) as a function of time. Contrast agent concentration = 300 mg/ml, injected volume = 1 ml.

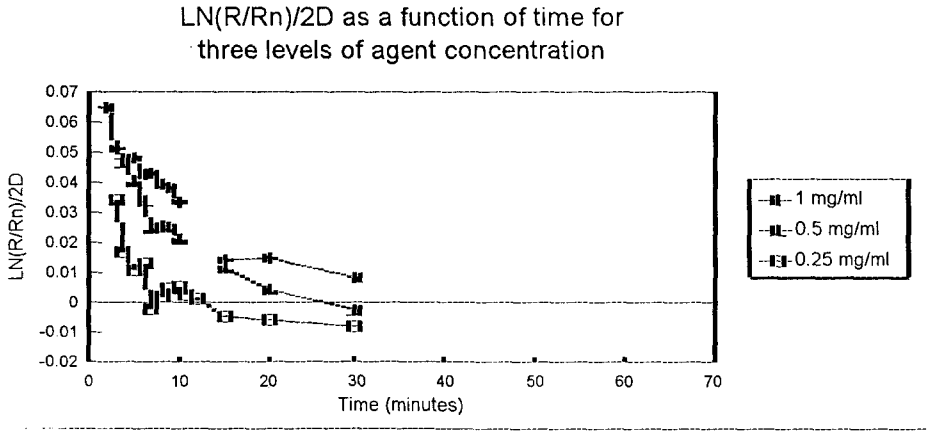

Figure 15: *In vitro* shadowing experiment - see theoretical development for explanation of LN(R/Rn)/2D parameter.

Received 2/8/2000

DEPARTMENT OF THE ARMY
US ARMY MEDICAL RESEARCH AND MATERIEL COMMAND
504 SCOTT STREET
FORT DETRICK, MARYLAND 21702-5012

REPLY TO
ATTENTION OF:

MCMR-RMI-S (70-1y) 21 Jan 00

MEMORANDUM FOR Administrator, Defense Technical Information Center, ATTN: DTIC-OCA, 8725 John J. Kingman Road, Fort Belvoir, VA 22060-6218

SUBJECT: Request Change in Distribution Statement

1. The U.S. Army Medical Research and Materiel Command has reexamined the need for the limitation assigned to technical reports written for the attached Awards. Request the limited distribution statements for Accession Document Numbers listed be changed to "Approved for public release; distribution unlimited." These reports should be released to the National Technical Information Service.

2. Point of contact for this request is Ms. Virginia Miller at DSN 343-7327 or by email at virginia.miller@det.amedd.army.mil.

FOR THE COMMANDER:

Phylis Rinehart

Encl
as

PHYLIS M. RINEHART
Deputy Chief of Staff for
Information Management